THE PENNSYLVANIA STATE UNIVERSITY
SCHREYER HONORS COLLEGE

DEPARTMENT OF FOOD SCIENCE

Effects of Sodium Citrate on Almond Proteins for Almond-Based Beverage Products

LEAH DOCTOR BODINGER
SPRING 2023

A thesis
submitted in partial fulfillment
of the requirements
for a baccalaureate degree
in Food Science
with honors in Food Science

Reviewed and approved* by the following:

Dr. Federico Harte
Professor of Food Science
Thesis Supervisor, Honors Advisor

Dr. Christopher Sigler
Assistant Teaching Professor/Academic Advisor
Faculty Reader

* Electronic approvals are on file.

ABSTRACT

High protein plant-based beverages are not inherently stable and require the addition of stabilizers and emulsifiers to ensure that proteins and other components do not settle out of solution, thus improving product acceptability. Emulsifying salts such as sodium citrate, potassium citrate, and dipotassium phosphate are added to dairy products to cause the dissociation of protein quaternary structures, improving product stability and functionality. The plant-based alternative industry's $22.6 billion value will double by 2040, causing research in this area to become increasingly important. A Continuous Monitoring Unit (CMU) was designed to monitor the effects of increasing concentrations of sodium citrate and temperatures on the turbidity and rheological properties of reconstituted and filtered almond protein dispersions. The CMU simultaneously measured changes in the solution's pressure, fluorescence, and absorbance values with increasing temperatures. Additionally, SDS-PAGE gel electrophoresis was used to analyze and identify protein subunits. Increasing the salt concentration from 0.1-100 mM was found to disrupt the quaternary structure of the almond protein, as higher concentrations of some protein subunits were present, but the type of protein changed. As seen via electrophoresis, the appearance of low molecular weight subunits decreased, while higher weight subunits became twice as pronounced. This trend was not as prominent with other parameters, as viscosity and fluorescence each changed by less than 0.5% throughout the series of salt concentrations. While the type of protein aggregate present in solution changed with increasing concentrations of sodium citrate, its effect on protein functionality, such as foaming and emulsification, remains unknown. As almond based beverages continue to rise in popularity, this work begins to fill the current gaps in knowledge within the plant-based food space but leaves further questions.

TABLE OF CONTENTS

LIST OF FIGURES

LIST OF TABLES

ACKNOWLEDGEMENTS

I would like to sincerely thank my thesis advisor, Dr. Federico Harte, for his guidance and advice over the past three years as I've worked in his Dairy Protein Laboratory as an Undergraduate Research Assistant. From the start, Dr. Harte welcomed me into his laboratory and encouraged me to become more involved with hands-on research studies, even during the COVID-19 pandemic when laboratory time and involvement were limited. Dr. Harte provided both academic and personal guidance during this time, especially when I was frustrated with a lack of scientific results or overwhelmed with responsibilities. Dr. Harte pushed me to grow as an individual during this time, encouraging me to trust my own decisions and to become more self-reliant. I am truly grateful for his positive attitude and kind nature!

Additionally, I would like to thank my mentor, Dr. Grace Lewis. I originally met Grace when she presented her graduate research project from Dr. Harte's lab during my freshman seminar course and admired her intelligence and ability to thoroughly explain the details of her work regarding the high-pressure jet and dairy protein processing. I was inspired to learn more about this technique and am so lucky to have shadowed her extensively as I learned how to conduct individual laboratory experiments. Grace taught me proper lab techniques, problem-solving, and scientific writing. Along the way, I became grateful for her advice as a young professional, incredibly strong woman, and role model within the scientific field.

Again, I am so grateful for the support and knowledge provided by both Dr. Harte and Dr. Lewis. I truly would not have succeeded in completing this senior thesis without their continuous patience and help.

Chapter 1

Introduction

Although dairy milk has been widely consumed for centuries due to its nutritional benefits, recent trends shown a decrease in the global consumption of dairy milk.[1] Individuals are leaning toward plant-based alternatives for their perceived health, environmental, or allergen purposes, especially as the prevalence of lactose intolerance increases and the link between dairy consumption and cardiovascular diseases remains controversial.[2] Due to these trends, the dairy alternative industry is expected to double its current value of $22.6 billion by 2040.[3] These plant-based fluids are meant to mimic dairy milk and are typically white in color with a "creamy" mouthfeel.[1] Plant-based beverages are created by grinding a plant base, soaking the ground powder in water, and homogenizing the solution to reduce its particle size. Plant-based beverages are not inherently stable and require the addition of stabilizers and emulsifiers to ensure that proteins and other components do not settle out of solution, thus improving product acceptability and customer usage. Emulsifying salts such as sodium citrate, potassium citrate, and dipotassium phosphate are added to dairy products to cause the dissociation of protein quaternary structures, improving product stability and functionality.[4] This research had been conducted using a recently developed instrument known as the Continuous Monitoring Unit (CMU) to simultaneously measure the changes in solution pressure, fluorescence, and absorbance with increasing temperatures.[5] However, the use of the CMU was not consistent as a standard operating procedure (SOP) had not been developed. The initial goal of this work was to

create a thorough SOP for the experimental and cleaning procedures, as well as troubleshooting potential issues, to guide future use of the CMU.

While the effect of emulsifying salts on the stability of dairy proteins has been widely researched, their influence on non-dairy beverage solutions is not well known. The ingredient labels on non-dairy "milks" often disclose the presence of emulsifying salts such as dipotassium phosphate, tricalcium phosphate, potassium citrate, and sodium citrate with claims that these additions help to maintain quality and prevent separation.[6] Although these compounds are widely used within industry, the solubility of most in water is limited. The scope of this work focused on the use of sodium citrate, as it has better recorded solubility in water and had performed well in previous research done by the Harte lab.[5] In addition to the different salts present, almond varieties and protein extraction protocols can affect the nutritional composition of the final product, possibly affecting its stability.[6] Testing different protein powders, salt concentrations, and a variety of temperatures would be incredibly time consuming if done individually, but the CMU provided a mechanism to automate this experimental design. The SOP for the CMU was completed simultaneously with experiments performed for each of three different almond protein powders to determine the effects of sodium citrate on almond protein stability and protein aggregation, as measured by fluorescence, absorbance, and viscosity.

Problem Statement

The effects of emulsifying salts at ranging concentrations on the turbidity, rheological properties, and soluble protein content of almond protein powder (APP) dispersions prepared from three commercial sources are currently unknown, hindering its use as a functional ingredient of the food industry. As an emulsifying salt, sodium citrate (SC) is hypothesized to disrupt the protein structure present by interfering with quaternary interactions rather than the amino acid primary sequence. The Continuous Monitoring Unit (CMU) prototype was used to test the interactions at increasing temperatures of varying SC concentrations with commercial almond protein powders via fluorescence, absorbance, and viscosity data.

Chapter 2

Continuous Monitoring Unit (CMU)

While other means of measuring the effect of ranging ionic conditions and temperatures on solutions existed, they were inefficient at measuring multiple variables at once. The Continuous Monitoring Unit, or CMU, was developed over the course of two years in Dr. Federico Harte's Dairy Proteins Laboratory at the Pennsylvania State University. This instrument was meant to measure the absorbance, fluorescence, and viscosity of protein dispersions simultaneously, increasing usability in the research laboratory setting and reducing the time needed to finish experiments. Once complete, it was used successfully to characterize the interactions of casein proteins with increasing ethanol concentrations, as published by Lewis et al. (2022) within the Harte lab.[5] The CMU allowed for optimum ethanol concentrations and temperatures to be determined for to fully disperse casein proteins. Following this publication, the CMU was also used within the lab to experimentally test the effect of emulsifying salts on plant-based proteins, beginning with soy protein isolates. However, as members of the Harte lab moved on from Penn State, knowledge of the CMU needed to continue beyond their graduation to pass down to future lab members and spread to other academic institutions internationally for further experimentation. As a result, the standard operating procedure (SOP) for the CMU was written and revised for clarity and purpose.

Continuous Monitoring Unit Mainframe

The CMU mainframe is the space where each sample travels through to be mixed and then analyzed. The mainframe tubing is mostly made of smooth seamless smallbore 1/16″

stainless steel with A-grade high-pressure connections to avoid leaks. The casing of the mainframe is Polyvinyl chloride (PVC), which is sturdy and insulating for proper temperature control of the samples. The path through the mainframe **(Figure 1 & 2)** is discussed in detail below:

Three LC pumps regulate the flow of the concentrated protein solution (stream 1; pump 1/Protein Pump, P1), a concentrated salt solution (stream 2; pump 2/Salt #1, P2), and de-ionized water (stream 3; pump 3/Buffer Pump, P3) **(Figures 1 & 2)**. Additionally, the CMU is equipped with a fourth pump (P4/Salt #2) for experiments that test the effects of multiple salts or solutions. In most experiments, the flow rate of pump 1 remains constant and the flow rate of pumps 2 and 3 are variable to achieve a desired salt content in the final samples that travel through the system.

After the pumps, the tubes for each stream pass through a heat exchanger connected to a digitally controlled temperature water bath (Poly Science AP07R-20-A12E; Niles, IL). The three streams are brought to the desired temperature and then enter the mixer (Cytiva 28956246 Mixer chamber 5mL; Marlborough, MA). The mixed sample passes through a flow cell for an absorbance measurement (Ocean Optics FIA-USP-100; Orlando, FL) via a light source (Ocean Optics Deuterium-Tungsten Halogen UV-Vis-NIR Light Source; Orlando, FL) and detector (Ocean Optics SR Series Spectrometer; Orlando, FL), a flow cell for fluorescence measurement (Ocean Optics FIA-SMA-FL-ULT; Orlando, FL) connected to a light source (Ocean Optics LED-VIS-KIT; Orlando, FL) and detector (Ocean Optics QEPRO-UV-VIS; Orlando, FL), and a pressure sensor to estimate viscosity (Omega PX409-050GUSBH; Norwalk, CT). The flow by the pumps as well as the signals by the spectrometers and pressure sensors are controlled and recorded by a computer equipped with LabVIEW software (National Instruments; Austin, TX).

The path of each sample in the mainframe starts with the combined liquid sample stream consisting of protein, salt, and water entering through a shell-and-tube heat exchanger (not pictured, bottom of the mainframe box in an insulating foam). The water bath **(#1, Figure 1)** brings the temperature of all streams to the desired level. Then, the set amount of dilution buffer (usually water) is mixed with salt #1 and salt #2 (if used) in the first cross connector (**#2, Figures 1 & 2**). Then, the designated salt concentration meets the protein solution in the second cross connector **(#3, Figures 1 & 2)**. One end of this second connector in attached to the first check-valve (**#4, Figures 1 & 2**). If the mixture forms a gel from a salt-out or an extreme temperature destabilizing the protein solution, the check valve opens at 20 psig (adjustable from 5-100 psig by the screw at the bottom that pushes or releases the spring inside). This prevents the excess pressure from building up further in the mainframe path. If that happens, the bypassed mixture (probably gel-like with a high viscosity) exits through a tube escape into the sink. This line must be empty and clean in order for the system to work properly.

The combined liquid sample (from the three streams) continues to flow into a magnetic mixer connected to a stirrer plate (**#5, Figures 1 & 2**) with a rotating magnetic stir bar that ensures the mixture becomes a homogenous sample for analysis.

Next, the homogenous sample flows to its first measurement in the pressure transducer (**#6, Figures 1 & 2**). The transducer is housed in a large tee connector facing upwards within the mainframe (Omega model # PX409; www.omega.com). The pressure difference (gauge pressure in psig) between the point of the transducer (**#6, Figures 1 & 2**) and the very end of the line allows for the estimation of the dynamic viscosity of the flowing liquid by the Hagen-Poiseuille equation.

Once the sample leaves the pressure transducer, it passes through another tee connector that introduces the high flowrate CIP streams from the CIP pumps (**a, Figure 2**). The CIP lines are equipped with backflow prevention valves to prevent backflow to the CIP pumps from occurring. The sample next enters the turbidity flowcell (**#7, Figures 1 & 2**). The UV-Vis beam from the deuterium lamp transverses the sample on the flow cell and then hits the spectrophotometer for detection.

After the turbidity flowcell, the sample moves into the M-cell for fluorescent spectroscopy (**#8, Figures 1 & 2**). Here, the excitation beam (280 nm for intrinsic L-Try or 385 nm for extrinsic ANS fluorescence) introduced from the fiber optic (600 SR) meets the sample at the exit of the cell and travels against the flow to hit the dark M wall. The emission beam is collected via the fiber in the back which enters the QE65 Pro detector. Since the volume inside the M-cell is 30 µL, a 30 µL/min flowrate of the same composition of each sample is kept during the spectroscopy measurements.

The fluorescence spectroscopy measurement is the last to be performed. The sample leaves the M-cell and heads into the last tee connector which hosts another check-valve to increase the gauge pressure measurements and therefore boost the sensitivity in detecting any weak gels that form in the system. The sample exits the mainframe from the left side through the waste tube and is disposed of into a sink.

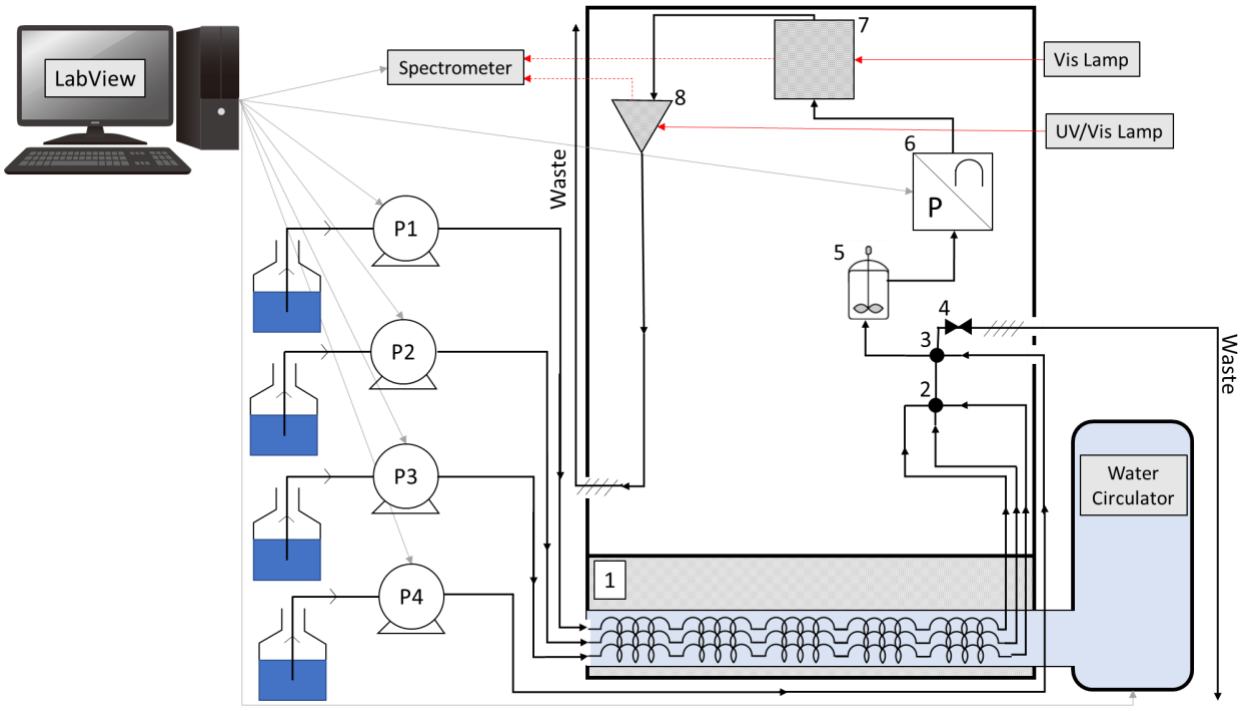

Figure 1. Schematic of the CMU showing flow of each pump, the Mainframe unit, and connected software

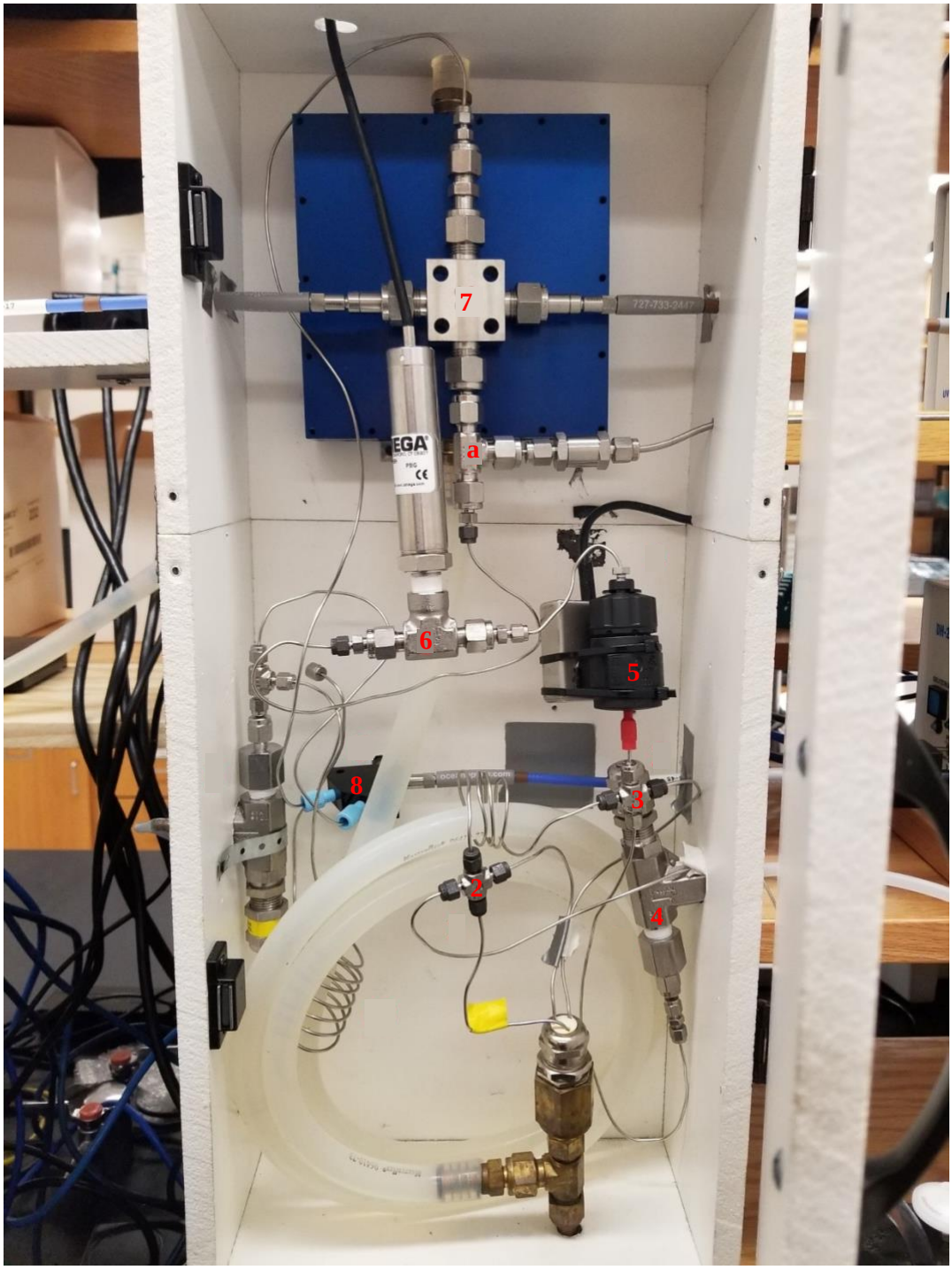

Figure 2. The CMU Mainframe.

#1 = Waterbath (not pictured), #2 = first cross connector (merging point of buffer and salt solutions), #3 = second cross connector (protein solution meets diluted salt solution), #4 = check valve (with exit if necessary), #5 = mixer, #7= turbidity flowcell, #8 = M-cell for fluorescence spectroscopy, a = third cross connector (where CIP system enters)

"Handshaking" Procedure

1) Open "WB + Pump Boot System" on the main screen of the computer desktop
2) Click "Turn Off Pumps and Water Circulator, then click here"
3) Turn on waterbath (flip switch in rear) and all 4 LC pumps (black switches on lab shelf)
4) Check list on computer to make sure each pump and waterbath is listed in top list as pictured in **Figure 3**
5) Close window on computer
6) Connect the detector for the absorbance flow cell by plugging in the black cable above the waterbath to the small black box connected to the mainframe

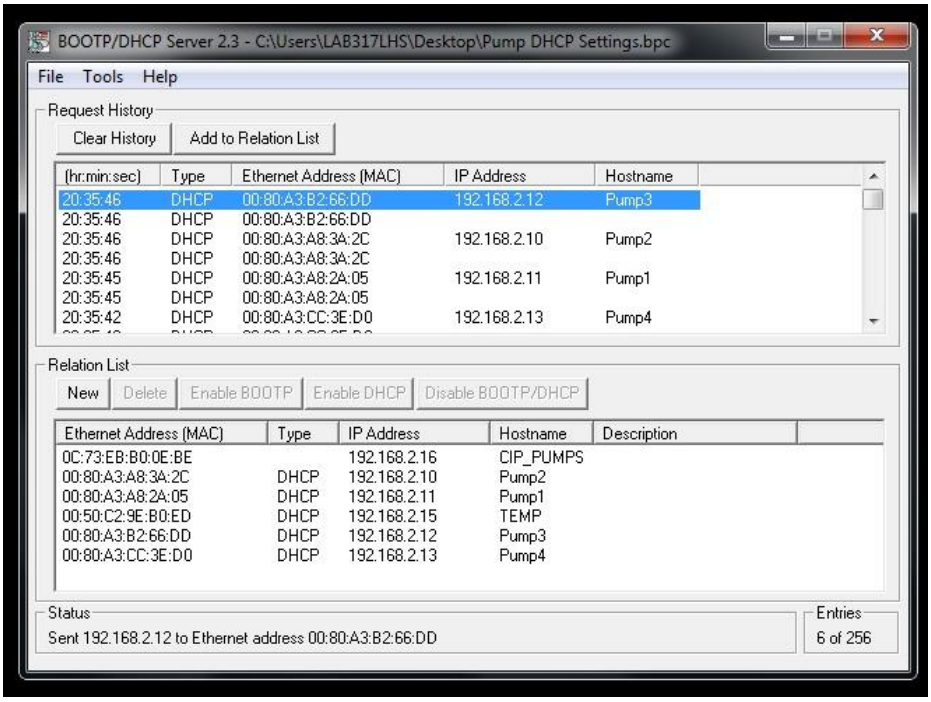

Figure 3. The BOOTP portal to initialize the pumps and the water bath.

Opening Software

1) Open "Behzad Labview" on desktop
2) Click "Labview folder"
3) Click Ver.1.411 folder (most recent)
4) Click CMU_Labview (main). The LabVIEW software has three tabs: parameters tab **(Figure 4)**, graphs tab **(Figure 5)**, and CIP tab **(Figure 6)**.

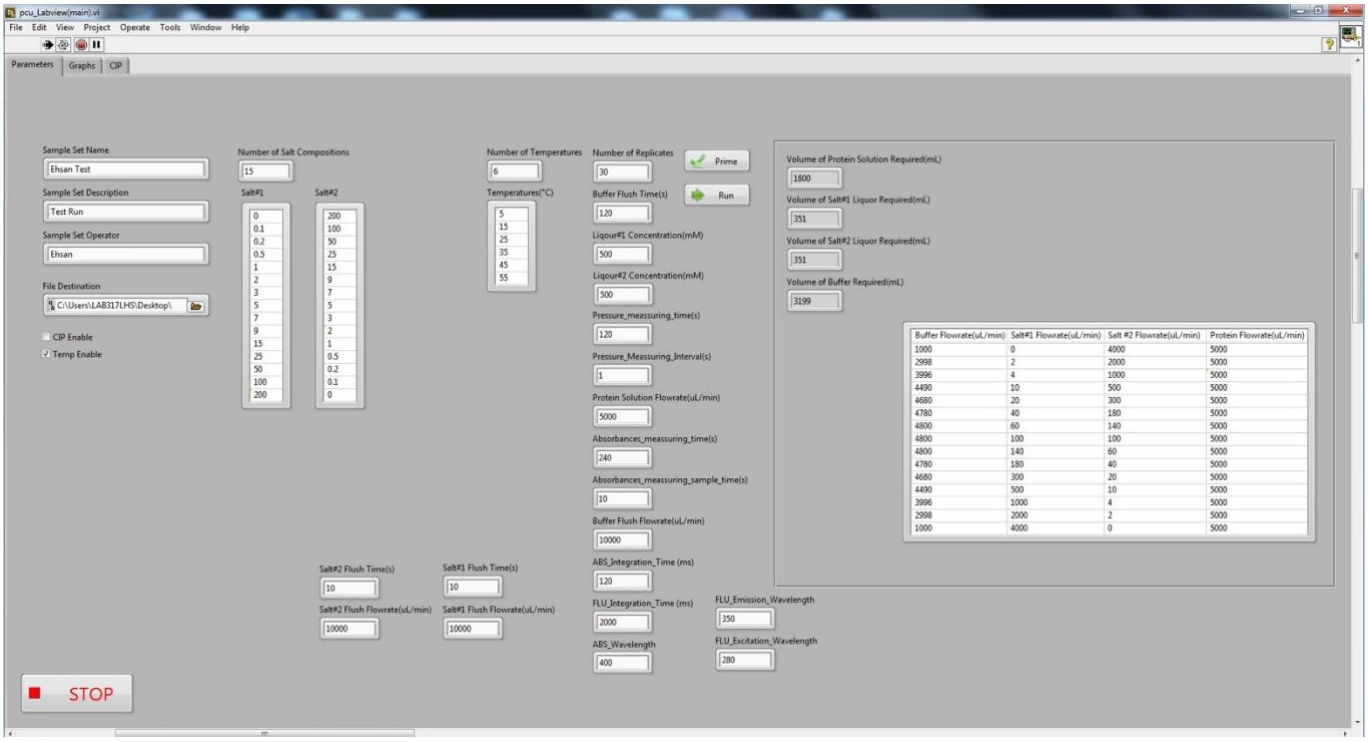

Figure 4. LabVIEW main VI parameters tab.

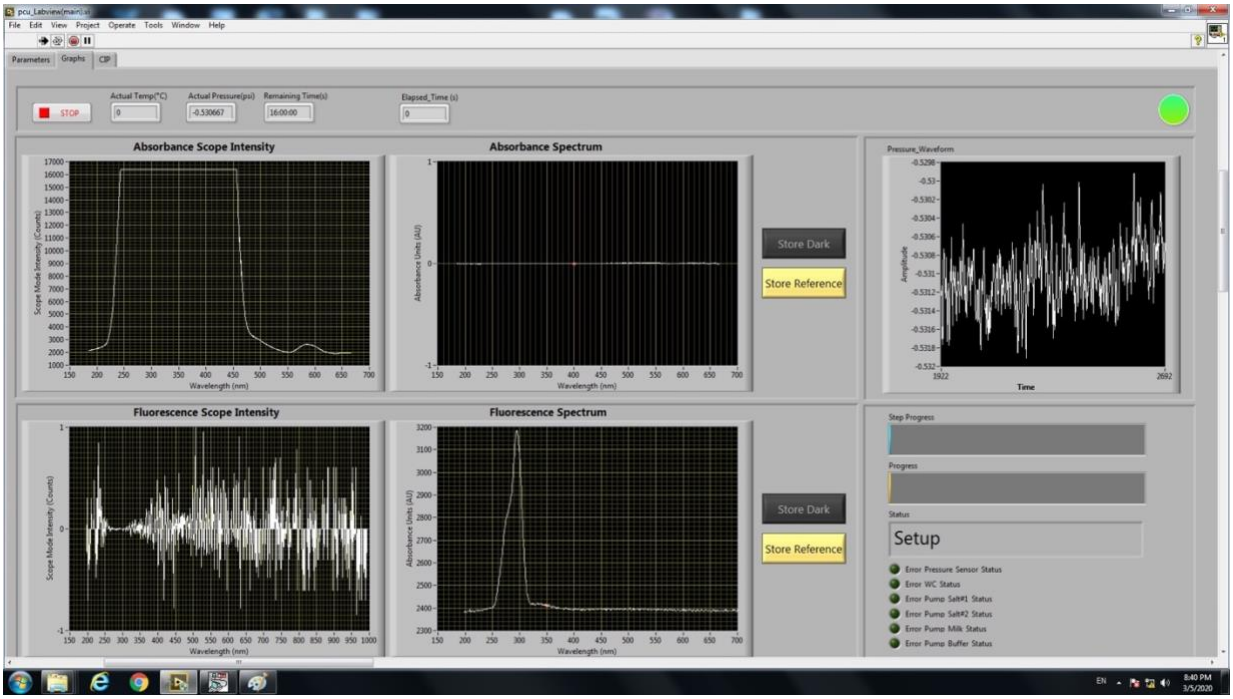

Figure 5. LabVIEW main VI graphs tab.

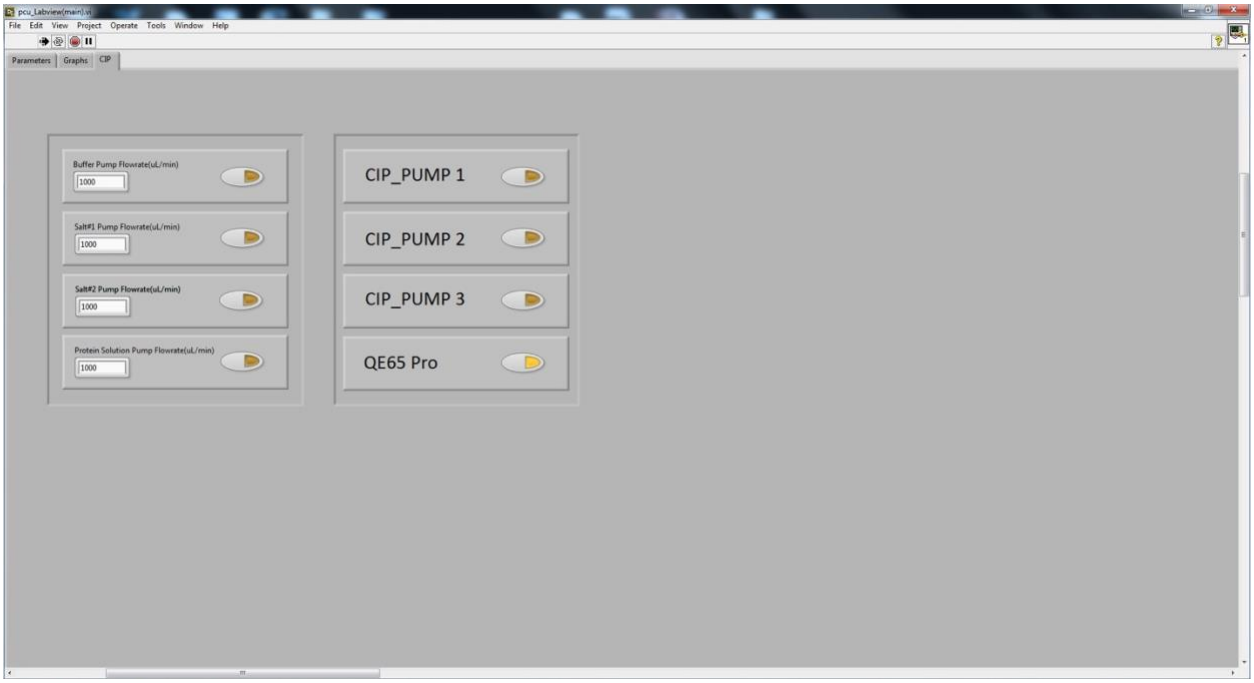

Figure 6. LabVIEW main VI CIP tab.

Starting Software

This step ensures that the software is prepared to run the sample when the proper parameters are set. It warms up the waterbath and prepares the system software to run once the lines are primed.

a. On parameters tab, click “Run” (top left corner of screen)
b. Check “Temp Enable”
c. Press Stop
d. When available, click “Run” again

Starting the Mainframe

1) Prepare the waterbath
    a. Set the correct starting temperature on the waterbath (use the physical Set button and up/down arrows on the screen, **Figure 7**) and add an ice pack if necessary (i.e., to cool waterbath faster)

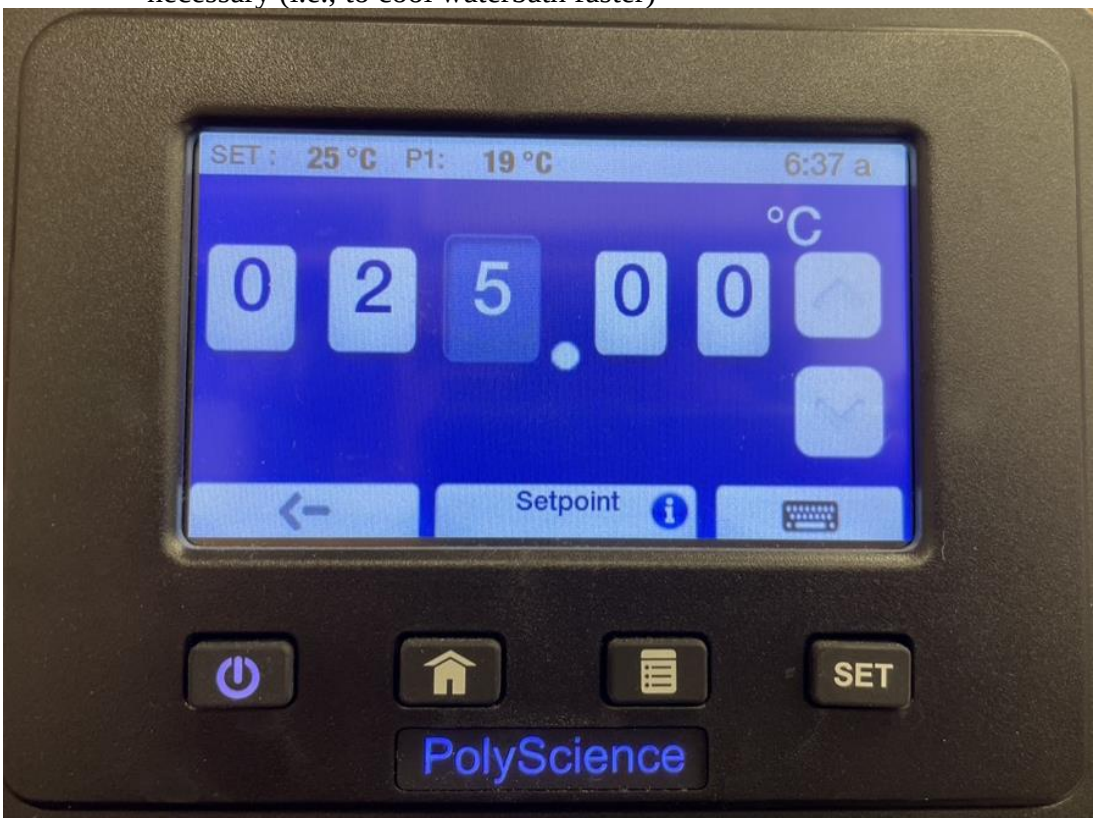

Figure 7. Waterbath Temperature Controls

2) Turn on the mixer (**Figure 8**; inside Mainframe) by turning the dial from horizontal (pictured) halfway until needle faces vertically downward

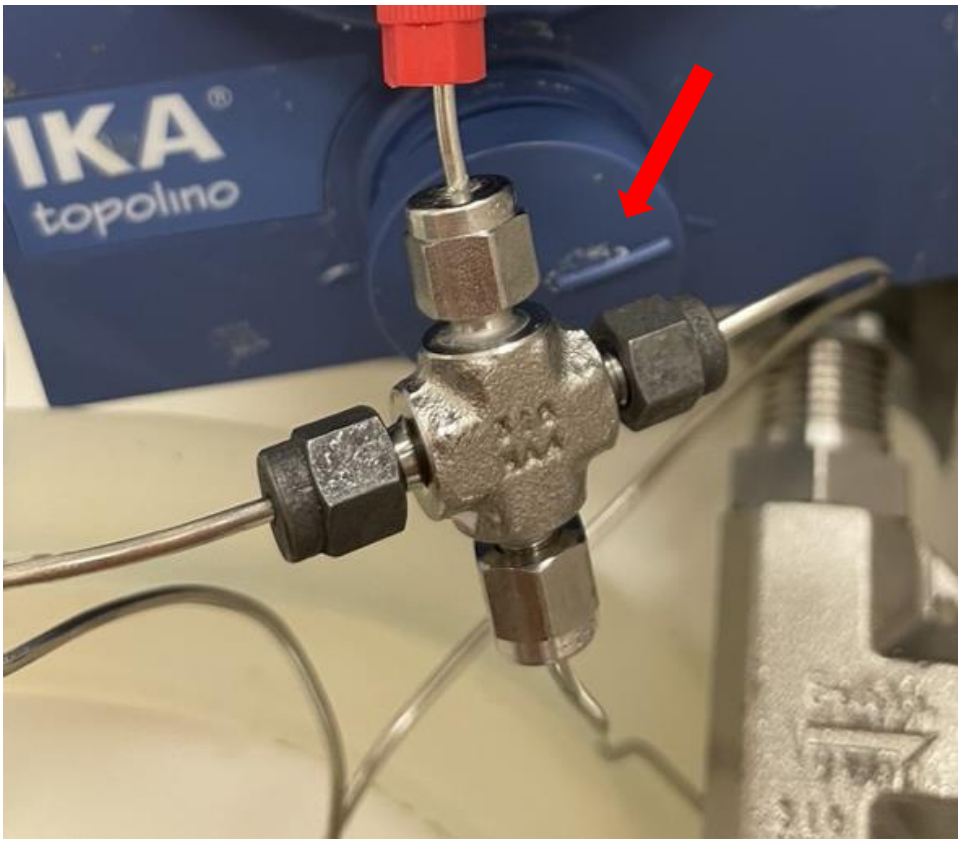

Figure 8. Internal Mixer, Off Position

3) Turn the fluorescence light source on at 35% power (210 mA) (**Figure 9**; flip black switch on left side, then power button)

Figure 9. The LED source controller for fluorescence spectroscopy.

4) Turn on the absorbance light source **(Figure 10)** by flipping the power switch in rear **(Figure 11).** Then press the blue “Deuterium” button on the front of the light source.

Figure 10. The deuterium light source for UV-Vis spectroscopy.

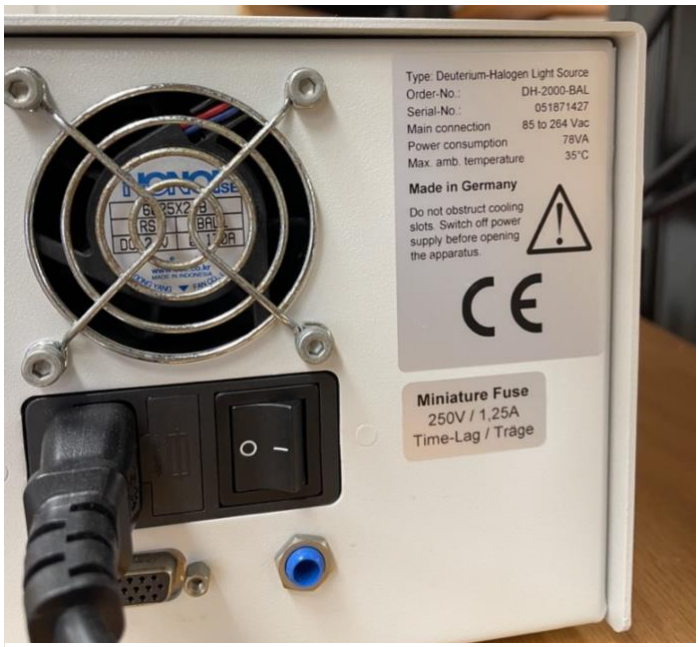

Figure 11. Power Switch for Fluorescent Light Source

5) Continue by connecting the cord of the fan to the black box located directly behind the mainframe **(Figure 12)**

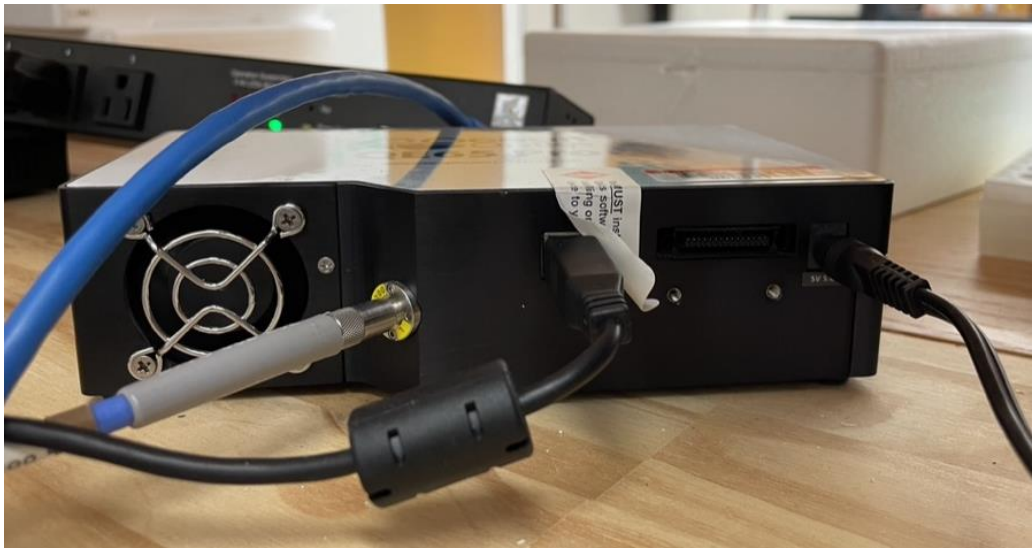

Figure 12. Fan with Power Cords Attached

6) Finish by filling the large water jug (top shelf) and open by changing the direction of the switch **(Figure 13)** from off to on

Figure 13. Water Jug in Off/Closed Position

Priming the Pumps

a. Transfer all pump lines to solutions needed for experiment (carefully to avoid bubbles in lines)
b. In CIP tab of software, turn on Buffer, Salt #1, and Salt #2 lines at 1,000 µl/minute, checking the Graphs tab for pressure to spike and level out between each addition **(Figure 14).** Run all 3 pumps (i.e., buffer, salt #1, salt #2) for 10 minutes.
c. After 10 minutes, turn off pumps for both Salt #1 and Salt #2.
d. Turn off the Buffer pump, increase flow rate to 10,000 µl/minute, and turn back on (check pressure spike). This is to clean all salt from CMU lines.
e. Start the protein pump at 1,000 µl/minute. Prime the Protein pump for 10 minutes, turn it off, and allow the buffer pump to continue for 5 additional minutes to clear the system.

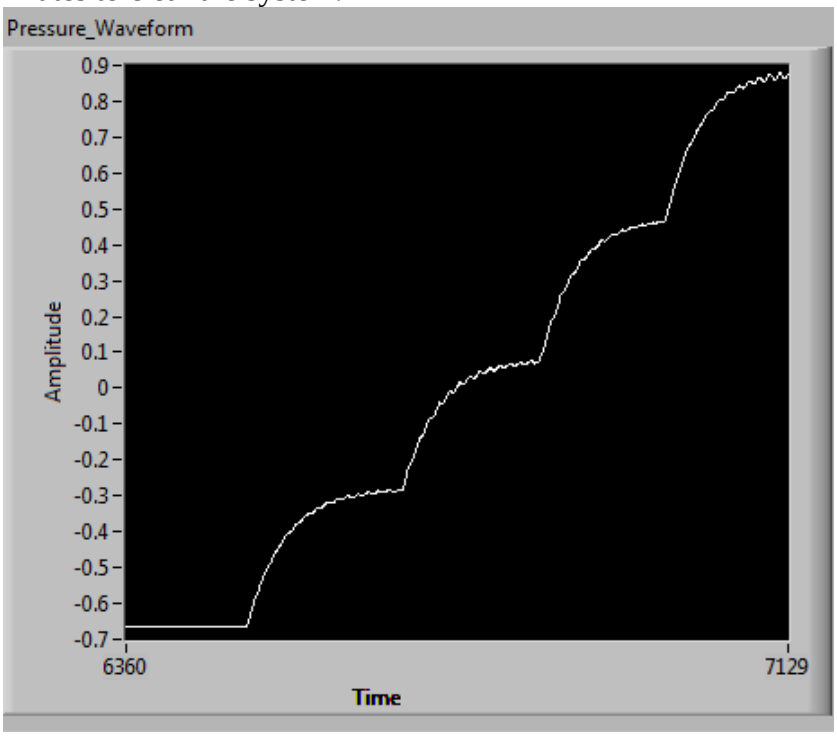

Figure 14. A healthy read on the pressure transducer when each pump is given 1 mL/min flow from static mode one after the other.

Setting the Blank for the Light Sources

f. With the Buffer pump still flowing, click on the "Graphs" tab of software.
g. Close the Absorbance light source by flipping the small metal switch on the front of the box to the "Closed" position **(Figure 15a)** and hit "Store Dark" 3 times on the software. Open the Absorbance source (flip the switch back to the starting position, **Figure 15b**) and click "Store Reference" 3 times.

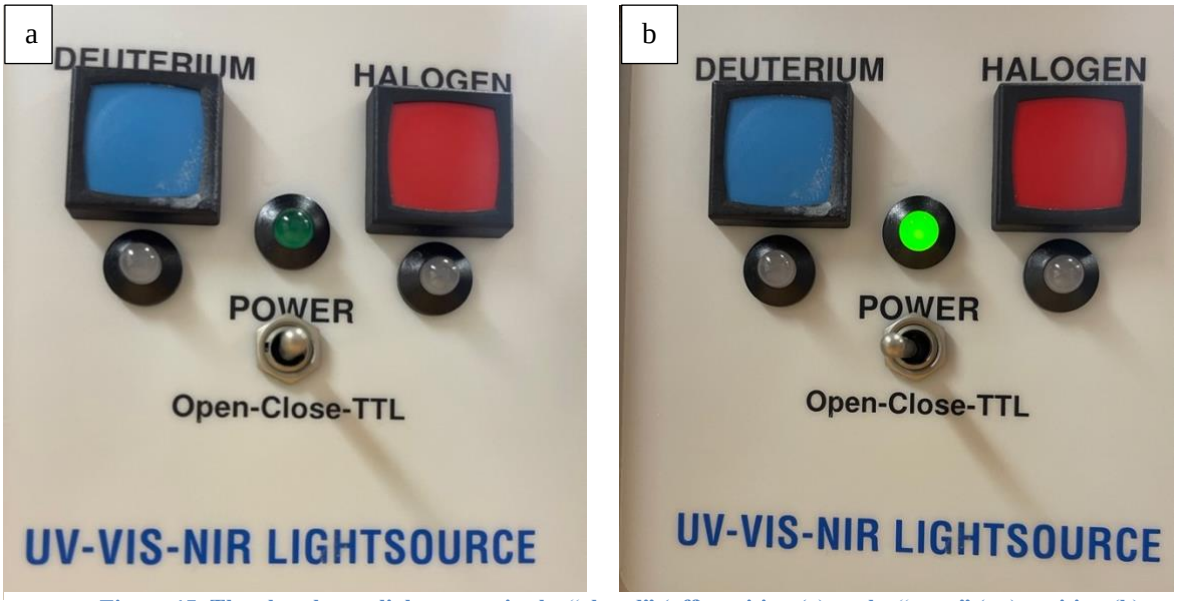

Figure 15. The absorbance light source in the "closed" (off) position (a) vs the "open" (on) position (b)

h. Click the power button on the Fluorescence home screen and hit "Store Dark" on the software 3 times. Turn the power button back on from the Fluorescence home screen (bottom left corner) and click "Store Reference" 3 times (wait between pressing the button each time).
i. Ensure proper calibration by confirming the Spectrum and Scope Intensity graphs as seen below in **Figure 16**.
    i. The Absorbance Scope Intensity should peak on the y-axis around 2400 counts for intensity at the matching coordinate for the set x-axis wavelength, before dropping to an x value near 0.
    ii. The Absorbance Spectrum should be a flat line for most of the range of the x axis, including the small red dot for the set wavelength. Variation on either/both ends of the spectrum is acceptable.
    iii. The Fluorescence Scope Intensity graph should appear similarly to the Absorbance Spectrum, centering around the set Fluorescence wavelength with acceptable variation corresponding with increasing distance from the wavelength.
    iv. The Fluorescence Spectrum should peak before the set wavelength for fluorescence, falling to a value of about 2,400 AU.

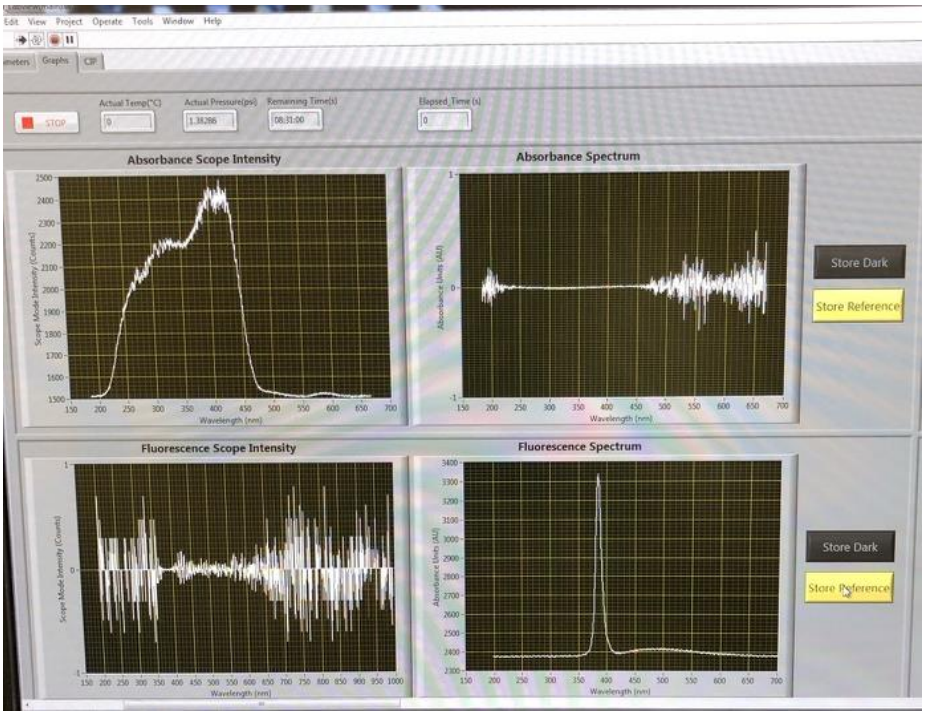

Figure 16. Calibrated absorbance and fluorescence spectroscopy graphs

Setting Parameters

j. When the waterbath reaches the correct temperature, remove the ice pack (if applicable)
k. Click the Parameters tab to determine and set correct parameters for the procedure **(Figure 17)**.
    i. Set the names for the Sample Set and input Sample Set description and operator.
    ii. Input the number of salt compositions and the concentration for each in the table below the heading.
    iii. Enter the number of temperatures tested and what each should be (°C)
    iv. Enter the concentration of both salts (0 for Salt #2 if only 1 salt is being tested)
    v. Input the Protein Solution Flowrate desired (typically 5000 uL/min)
    vi. Change the absorbance measuring time to 240 seconds.
    vii. Enter the FLU integration time (typically 2000 ms)
    viii. Input the desired absorbance wavelength used.
    ix. Change the fluorescence emission and excitation wavelengths to match the sample.

l. After pressing “Prime” on the “Parameters” tab of the software, ensure that each solution contains at least 200 mL more than the listed volume in the table on the righthand side of the screen (refill as needed).
m. Use the “CIP” tab to ensure all pumps are off.
n. Press “Run” under the “Parameters” tab.

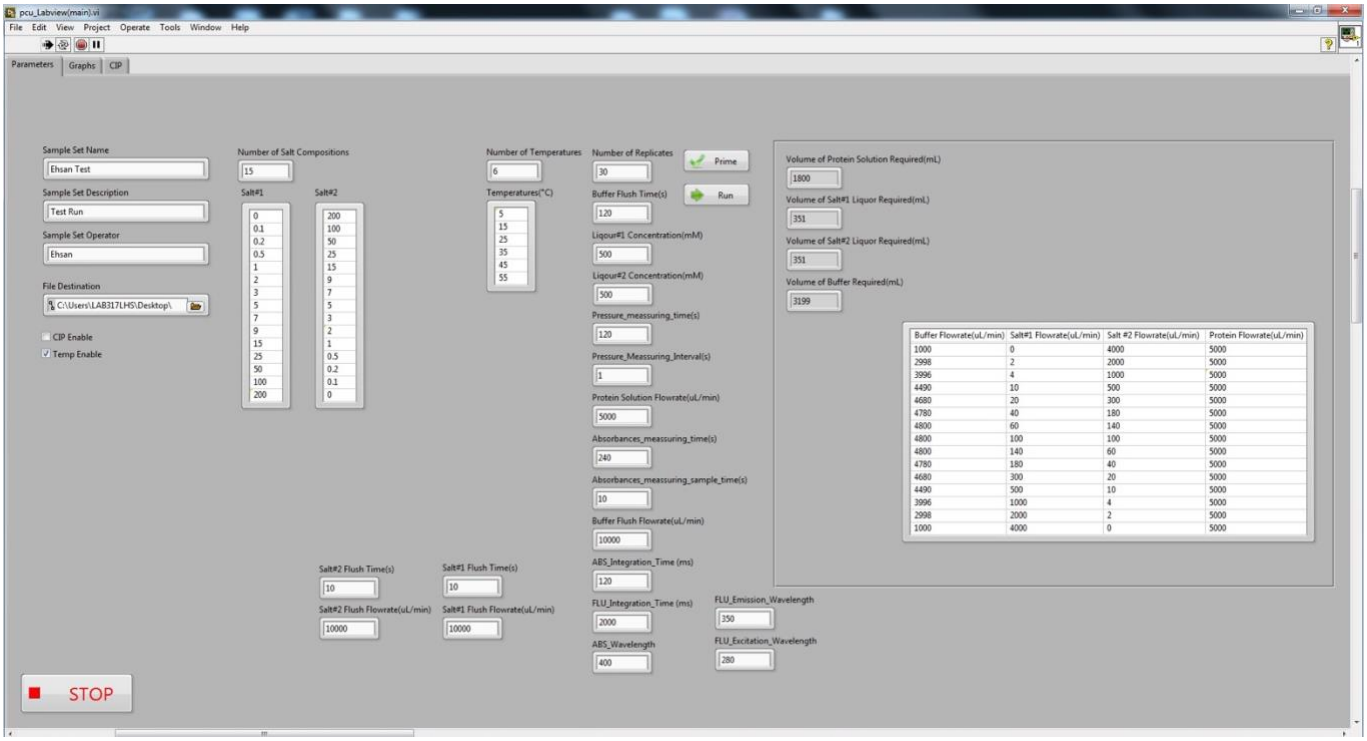

Figure 17. LabVIEW Parameters Tab with Run Settings Specified

Cleaning the Continuous Monitoring Unit

L.C. Pumps: Full Cleaning Procedure

Cleaning the Pump Heads and Lines to the Mainframe

1) Push “Run” (small white arrow in the top left corner) on the Labview software (parameters tab) and set the temperature to 25°C on the waterbath.
2) Ensure that all pumps are off.
3) Transfer the Protein pump line to a 1% Alconox solution and refill Buffer and Salt #2 pump solutions with DI water. Salt #1 should stay with the same salt solution.
4) Run all pumps at 1000 µL/minute by toggling each yellow button under the “CIP” tab on Labview. Start each pump separately and check the “Graphs” tab for a pressure spike between each addition as shown previously in **Figure 14**.
5) After all L.C. pumps have run at 1000 µL/minute for 30 minutes, turn each pump off using the “CIP” tab.
6) Transfer the Salt #1 line to DI water.
7) Start the Salt #1, Salt #2, and Buffer pumps all at 10,000 µL/minute using the “CIP” tab, ensuring that a pressure spike occurs on the “Graphs” tab between each addition.
8) Start the Protein pump at 2,000 µL/minute, checking for a pressure spike on the “Graphs” tab.
9) After 5 minutes, turn off the Salt #1, Salt #2, and Buffer pumps under the “CIP” tab.
10) Allow the Protein pump to run for at least an additional 30 minutes.
11) Turn off the Protein pump using the “CIP” tab and leave the system overnight with the Protein line still in 1% Alconox solution.
    a. Before leaving the system, turn off all pumps, the waterbath, the mixer, and both light sources. Unplug the fan and Absorbance connection and switch the water jug line to the off position.
12) After leaving the system overnight, begin with the “Handshaking” procedure (step 1 of SOP).
13) Once complete, start the Protein pump (still with 1% Alconox solution) at 5,000 µL/minute using the “CIP” tab.
14) After 30 minutes, stop the Protein pump and switch the line to DI water.
15) Start the Protein pump with DI water at 5,000 µL/minute, checking for a pressure spike on the “Graphs” tab.
    a. If necessary, other lines can be switched to experimental solutions at this point to start the Priming process.
    b. If no experiment is to be run, turn the Protein pump off after 30 minutes using the “CIP” tab. Switch all lines to ethanol storage solution.

Mainframe: Cleaning with CIP Pumps (can be done simultaneously with L.C. Pump Cleaning)

1) Ensure that CIP Pump 3 solutions are properly filled before continuing— CIP Pump #3 with 1% Alconox in DI water and CIP Pump #1 with DI water.
2) Run CIP Pump #3 with 1% Alconox for 5 minutes (toggle yellow CIP Pump #3 button under "CIP" tab). Check the "Graphs" tab to ensure a (very large) pressure spike occurs.
3) After 5 minutes, turn off CIP Pump #3 under the "CIP" tab.
4) Turn on CIP Pump #1 under the "CIP" tab to run with DI water. Check the "Graphs" tab to ensure a pressure spike occurs.
5) Turn off CIP Pump #1 after 5 minutes.

Shortened Cleaning: Cleaning the Pump Heads and Lines to Mainframe between runs.

1) Transfer the Protein Pump line to 1% Alconox solution. Check that the Buffer and Salt #2 stores are sufficiently filled with DI water and that Salt #1 has enough salt solution before continuing.
2) Run Protein at 10,000 µl/minute, Buffer (with water) at 1000 µl/minute, Salt #1 (still with salt) at 1000 µl/minute and Salt #2 (water) at 1000 µl/minute for 15 minutes.
3) Turn off Buffer, Salt #1, and Salt #2 pumps.
4) Run the Protein line for an additional 30 minutes at 10,000 µl/minute with 1% Alconox solution.
5) Change the Protein line to a solution of 50% ethanol and 50% DI water. Run Protein pump only at 10,000 µl/minute for 30 minutes.
6) Swap all pump lines to DI water and run all at 5,000 µl/minute for at least 10 minutes before stopping.

Note: You <u>must</u> do the mainframe cleaning if you do either the short or long cleaning

Pump Head Removal and Cleaning

1) Remove the water line connections from the top of the pump and unscrew the fluid lines from the bottom.
2) Use an appropriately sized Allen wrench to remove the pump head from the system. Carefully alternate between screws, ensuring that they stay even throughout.
3) Unscrew pump cover and remove all small parts.
4) Place all parts in a 1% Alconox solution and agitate for 1 hour or overnight.

Reassembly Process

1) Check to ensure that all parts pictured (**Figure 19**) are clean and ready for assembly.

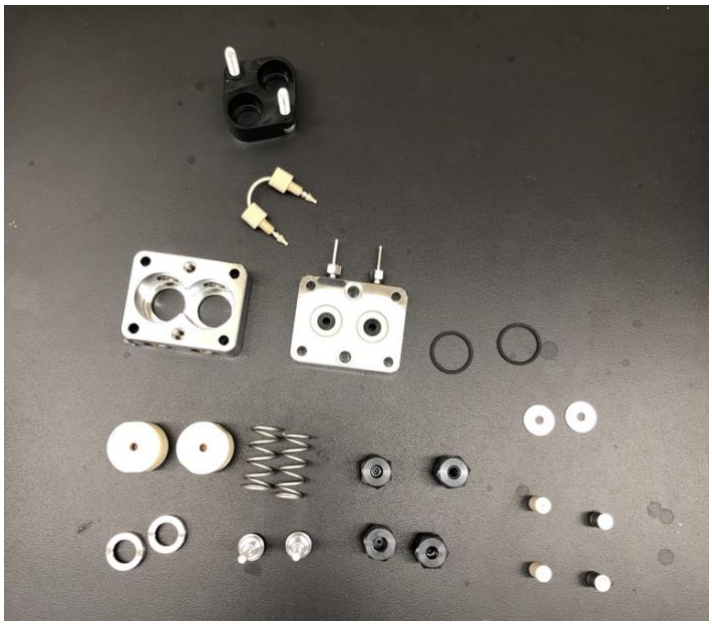

Figure 19. Pump Head Parts (disassembled)

2) Align labeled white plastic inner part in metal pump casing with words facing out and legible as seen in **Figure 20**.

Figure 20. Alignment of plastic inner pump within metal casing

3) Place small black disks in groove of back side of pump (see **Figure 21**).

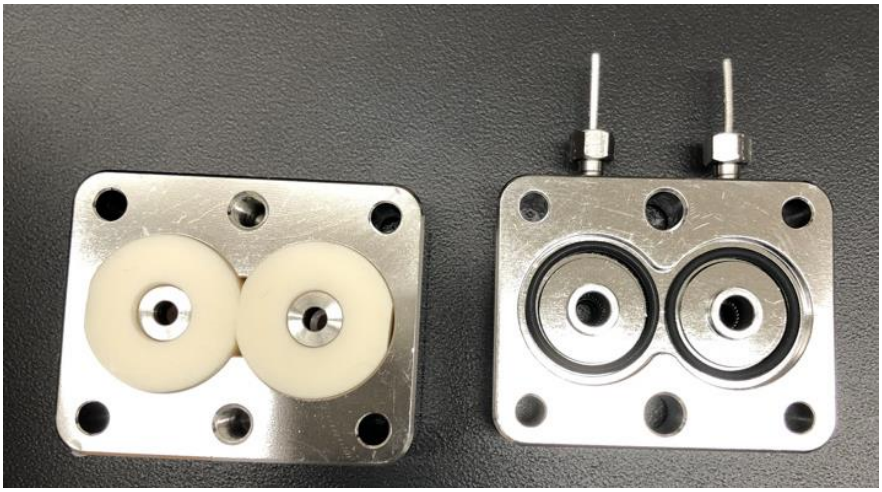

Figure 21. Front and back of metal pump casing

4) Place both halves of pump casing together and align pump casing top and bottom sides **(Figure 22)**.

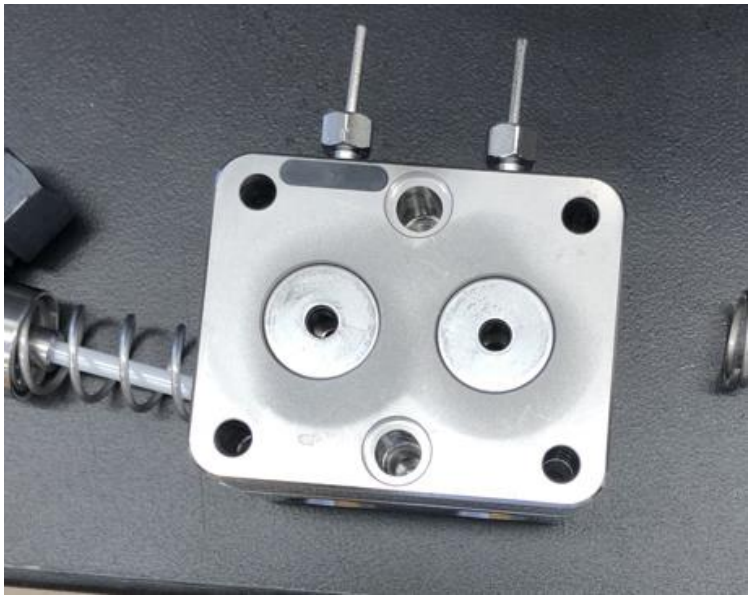

Figure 22. Aligned pump casing

5) Place large screws on top of pump casing openings with silver metal heads balanced on top **(Figure 23)**.

Figure 23. Placement of Large Screws and Screw Heads

6) Place black diamond-shaped black plate on top of large screws and insert small screws on both sides vertically **(Figure 24)**.

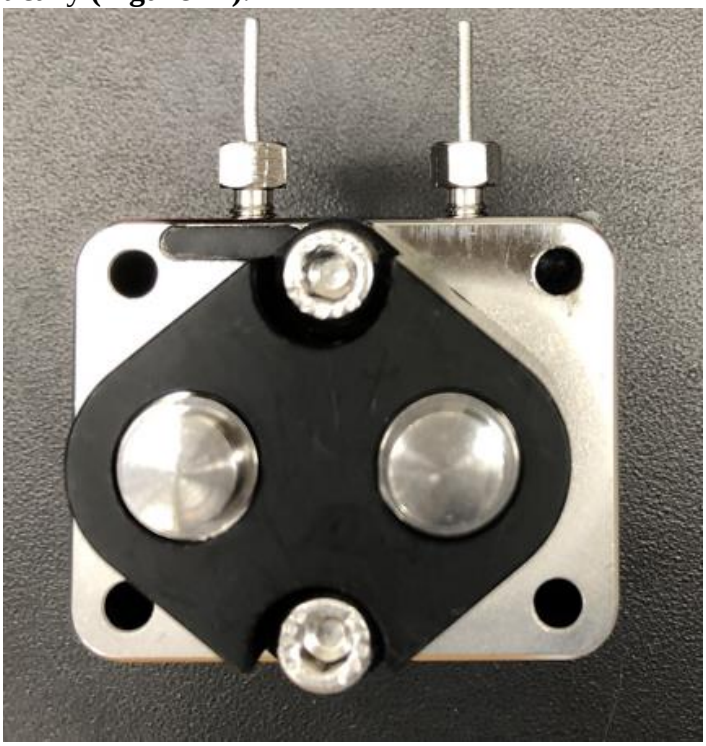

Figure 24. Black plate and small screws inserted

1) Tighten screws with an appropriately sized Allen wrench, alternating between them to keep the distance approximately even.
2) When needed, reattach pump to pump head with four small screws, using the same L shaped tool to tighten in a zigzag pattern to ensure that screws don't get stripped.
3) Reconnect water lines on top of pump and attach black screws to bottom with torque wrench set at 5 Nm for stainless-steel fittings or 0.5 Nm for Peek fittings. Attach lines by screwing in underneath pump after pushing solution through using the syringe.

Troubleshooting

Table 1. Flow Issues

Problem	Possibilities
Head pumps are leaking from one or more tube entrance.	• The inlet/outlet is not screwed on well. • The nut in the pump head didn't get tightened to the correct torque. Loosen and re-tighten to ensure proper torque. • The check valves might be in the wrong place or direction or be clogged. Remove the check valves, clean (with agitation in 1% Alconox), and replace. The in/out adapters connecting the pumps to each line might break because of the plastic-metal connection. Check them periodically.
The head pump is leaking from the white circle in the middle.	The pump head is not tight enough and the seals are not working. Disassemble the pump head and re-assemble it correctly.
There is a bubble in one of the pump lines.	• Unscrew the line from the pump. Use a syringe with the correct solution and connect to the open end of the pump line. Push the solution through until no bubbles persist. With the syringe still connected, screw the pump line back in. Carefully remove the syringe and place the open end of the line back in the original solution. • Start the flow for the line at 10,000 µl/minute and check for a proper increase in pressure.

Table 2. Software Issues

Problem	Possibilities
When trying to start a new run, the program won't respond.	• The waterbath and/or the L.C. Pumps are not turned on. Check all connections and plugs. • Try turning everything off and on again, including all pumps and computer program. May need to try multiple times. • Do the "handshaking" procedure correctly. If the problem persists, there might be a connection issue.

Table 3. Pressure Issues

Problem	Possibilities
The pressure transducer shows pressure dropping.	• Make sure that there are no leaks in the Pump Heads. • Prime the pump to get rid of air bubbles.
When turning on a pump, no increase in pressure shows on the monitor graph.	• Make sure the outlet of the L.C. pump is connected. • Prime the pump to get rid of air bubbles. • Make sure that all the check valves are in their correct place and position. There is a chance that the pump will turn on but the motor will not work, change it if necessary.

Chapter 3

Almond Proteins in Ionic Environments

Introduction

Almond milk is the most popular non-dairy beverage in the United States, contributing over half of category sales annually by value.[7] Plant-based beverages are perceived to have health benefits as they are low in saturated fats, do not contain cholesterol, and are lactose free. In addition, their incorporation of bioactive minerals, vitamins, fiber, and antioxidants causes them to be commonly labeled as functional foods[1] with 41% of individuals perceiving almond milk to be healthier than its dairy counterpart.[8] As concerns for the environment and sustainably remain at the forefront of the consumer's mind, plant-based options provide an option to potentially leave a smaller carbon footprint than their methane-producing dairy equivalents.

In 2021, almond milk dominated the plant-based market holding over three-quarters of the share.[3] The health halo surrounding this nut (though scientifically categorized as a drupe) focuses on its lipid content, effect on the human immune system, and digestibility. Consumers perceive almond milk to be a lower-calorie alternative to dairy milk, especially as it contains only 30 calories per one cup (8 oz) serving when unsweetened. Additionally, the plant-based market suggests that almond milk is the most comparable to dairy milk in terms of taste, texture, and versatility in the kitchen, while also viewing it as a more sustainable alternative. Almonds are thought to provide a healthy fatty acid profile of primarily monounsaturated fats (oleic acid) linked to heart health, with lipids contributing to nearly half of their overall weight.[1] Additionally, almonds are a good source of alpha-tocopherol (Vitamin E), a powerful antioxidant able to help the body fight free radicals and prevent oxidative stress.[1] Almonds also contain

minerals such as magnesium, copper, phosphorous and other compounds including polyphenols and phytosterols.[1] However, due to its complexity and functional properties, the protein component was the focus of this study.

Almonds are approximately 16-26% protein by weight, with amandin serving as the key extractable protein component.[6] Amandin is a water soluble globulin with a hexameric structure and has a total molecular weight between 275-450 kDa.[6] Globulins are one of the main four protein categories determined by Osborne according to their solubility in different solutions, along with prolamins, glutelins, and albumins.[9] The structure of amandin includes both acidic and basic polypeptides with estimated molecular masses of about 40 and 20 kDa, respectively.[6] These subunits are linked with disulfide bridges, which help provide stability and structure but can be denatured by extreme heat or the addition of chemicals.[6] Other protein types within the almond are soluble in water, salt, and buffer solutions with a pH between 6-11.[6] This limited range in solubility complicates the manufacturing and stability of almond-based products, even as they reign as the champion of the plant-based market. Additionally, almond proteins can be extracted in multiple ways leading to products with contrasting attributes and protein profiles. Almond protein extraction is typically performed via either a traditional aqueous or an enzyme-assisted aqueous extraction process, where altering the amount of enzyme present affects the total amount of protein extracted from the whole nut.[6] Companies are not required to disclose the means of extraction for almond protein products and the United States Food and Drug Association (FDA) has not yet established a standard identity for almond or other plant-based milk, so variability between products remains high.

As consumers seek out clean label food products, the lengthy list of ingredients within almond milk fail to hit the mark. Almond beverages commonly contain thickeners such as gellan

and locust bean gums, oil sources (typically sunflower and/or canola) to improve texture and mouthfeel, and emulsifying salts such as potassium and sodium citrate for hypothesized protein stabilization. The true impact of these added stabilizers was unknown, especially the means of their interactions with the various protein subunits within plant protein isolates. This research examined the potential interactions of sodium citrate, a commonly used emulsifying salt within the plant-based industry, and a range of almond protein powders in order to determine the mechanism of stabilization. The CMU was used to automate the experiments for this data through multiple replicates and a wide range of temperatures and salt combinations, although it proved to be less reliable than initially perceived. Overall, sodium citrate was concluded to disrupt the quaternary structure of almond proteins, leading to the exposure of individual amino acids and monomeric units seen via gel electrophoresis and both increased fluorescence values and decreased viscosity as measured by the CMU.

Materials and Methods

Almond protein dispersion and salt solution preparation

As almond protein extraction protocols were unknown, multiple almond protein powders from different sources were tested to account for variability. Sources included 100% Almond Protein Powder Unflavored (APP 1; 60% protein based on Nutrition Facts content, Noosh; Simi Valley, CA), Organic Almond Protein Powder (APP 2; 53.6% protein, Lekithos; Tequesta, FL), and Almond Protein Powder (APP 3; 48.6% protein, Octonuts; Stockton, CA). All APPs were solubilized by continuous mixing of a 1% (w/w) solution of APP and distilled water at 40°C for 1 hour followed by refrigeration overnight at 5°C. Filtration was performed to remove insoluble solids using a 7 µm pore size filter (Whatman Grade 595 Qualitative Filter Papers, Cytiva Life Sciences; Marlborough, MA) and vacuum system before the dispersions were adjusted to pH 8 using 1M sodium hydroxide (NaOH). Sodium citrate (SC; CAS Number: 6132-04-3) from MilliporeSigma (Burlington, MA, USA) was solubilized to 250 mM while stirring. The pH of the salt solution was not adjusted in order to mimic its typical use in industrial settings.

Continuous Monitoring Unit (CMU) Mainframe

The body of the CMU includes four high-pressure LC Positive Displacement pumps (Knauer AZURA pump model P 2.1S, GMI, Ramsey, MN), each used to transport a different solution to the mainframe system for mixing and assessment. The capabilities of the mainframe, including the flowrate of LC pumps, temperature, spectrophotometer, and collection of resulting data were controlled via LabView software (National Instruments, Austin, TX).

A shell-and-tube heat exchanger connected to a water bath (Model PD07R-20-A11B, Polyscience, Niles, IL) within the CMU mainframe was employed to control the temperature of the solutions from 5-35°C, in 10°C intervals. The first cross connector mixed the solutions from Pump A (distilled water), Pump B (sodium citrate solution), and Pump C (APP dispersion) **(Figure 2. The CMU** Mainframe.**)**. Pump D was connected to a cleaning solution (1% w/v Alconox in distilled water) and was only used to flush the mainframe between samples, entering the unit at the second cross connector **(Figure 2. The** CMU Mainframe.**)**. In their path through the system, the combined solutions next reached the magnetic mixer (M-925 mixing chamber, 2 mL: Cytiva, Marlborough, MA) before continuing to the pressure transducer (model PX409, Omega, Norwalk, CT) and absorbance flow cell (Flowcel-1/2", Avantes, Louisville, CO). The flow cell was connected through fiber optics to a deuterium light source (DH-2000-BL, Ocean Optics, Largo, FL) and a spectrometer (STS-UV, Ocean Optics, Largo, FL).

The four lines of the LC pumps were primed as follows: Pump A with distilled water, Pump B with 250 mM sodium citrate, Pump C with 1% w/w APP dispersion, and Pump D with 1% w/v Alconox for cleaning. The flow rate of APP was kept at 5 $mL.min^{-1}$ to keep the samples at 50% (v/v) APP dispersion. To control the emulsifying salt concentration (0-25 mM sodium citrate), the CMU was programmed to adjust the flow rates of water (Pump A) and sodium citrate (Pump B) between 0 $mL.min^{-1}$ and 5 $mL.min^{-1}$. **Table 4** describes the variables monitored by the CMU, listing each time that was tested, the full temperature range for each time, and the salt concentrations added by Pump B with each combination.

Table 4. CMU Variables for Replications

Time (s)	Temperature (°C)	Salt Concentration (mM)
0	5	0
10	15	0.1
20	25	0.2
30	35	0.5
40		1
50		2
60		3
70		5
80		7
90		9
100		15
110		25
120		50
130		100
140		
150		
160		
170		
180		
190		
200		
210		
220		
230		
240		

Sample fluorescence (Emission 325 nm, Excitation 350 nm) was measured to characterize the aggregation and dissociation of APP components via the exposure of tryptophan residues[10]. The sample solution was held in the flow cell for 2 seconds. The data for fluorescence at 0 seconds was reported as the values were found to be most reliable between replicates.

Viscosity of the solution was measured, also at 0 seconds, by recording the sample pressure in the flow cell via the pressure transducer while the sample was flowing (Model

PX409, Omega, Norwalk, CT). As the solutions were expected to be Newtonian in nature with laminar flow, Poiseuille's equation (1) was employed to directly correlate pressure and viscosity:

$$\eta = \frac{(P_2 - P_1)\pi r^4}{Q8l} \qquad [1]$$

where η is the Newtonian viscosity, Q is the flow rate in the direction from high pressure (P_2, read from transducer) to low pressure (P_1 = 0 gauge pressure), tube radius = r, and tube length = l.

The percent coefficient of variation of both pressure and fluorescence readings was reported to give a more accurate representation of measurements as the precipitates formed with the addition of salt increased variation among consecutive measurement of absorbance and fluorescence.

Statistical Analysis

Three different types of Almond Protein Powders (APP 1, 2, 3) were tested to account for differences in APP origin and processing history. Of these types, three replicates of data from the CMU were chosen for analysis from a minimum of five replicates taken for each APP. Triplicates were chosen based on precision of compared attributes and success of the instrument and its measurement tools. Measurement analysis was performed through calculation of the average, standard deviation, and percent deviation from the mean.

$$\text{Percent deviation} = \frac{\text{Pressure or fluorescence at n mM}}{\text{Pressure or fluorescence at 0 mM}} \times 100$$

Ultracentrifugation

To prepare for further procedures, samples were ultracentrifuged to separate proteins to the supernatant. Any other components with higher density settled to the precipitate, improving the clarity of the supernatant and the results to follow. Each APP and salt solution combination (Table 4) was transferred to small tubes and ultracentrifuged (Sorvall MTX 150 Micro-Ultracentrifuge, Thermo Scientific; Waltham, MA) for 1 hour at 20°C at 60,000 x G using a S50-A 2056 rotor (Thermo Scientific; Waltham, MA).[11]

SDS-PAGE Gel Electrophoresis

SDS polyacrylamide gel electrophoresis (SDS-PAGE) under reducing conditions was conducted following procedures described in the BioRad manual (Laboratories Bio-Rad, 2012).[12] An aliquot of 10-µL sample buffer (0.5M Tris-HCl buffer at pH 6.8, 10% (w/v) sodium dodecyl sulfate (SDS), 2% (v/v) 2- β-mercaptoethanol, glycerol, and 0.5% (w/v) bromophenol blue) was combined with 10-µL of the ultracentrifuged sample and heated in a boiling water bath for 5 minutes. The samples were cooled to room temperature. Five uL of NativeMark LC0725 molecular weight standards (Invitrogen; Waltham, MA) were added to the first and last well of all 12% TGX precast gels (Bio-Rad Laboratories, CA) to provide a reference, as shown in **Figure 25.** Twenty uL of each sample was added to subsequent lanes within the gel. The gels were run at 200 V with 1X Tris/glycine/SDS running buffer to complete electrophoresis until the dye front reached the bottom of the chamber at approximately 35 minutes of run time. The gels were then stained with Coomassie Brilliant Blue R-250 Staining Solution (Bio-Rad Laboratories, CA) with agitation overnight. Following the staining procedure, the gels were rinsed with

distilled water and destained with ethanol/glacial acetic acid rinses until the bands were visible. Almond protein subunits were identified in reference to the protein standard ladder.

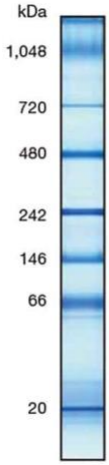

Figure 25. NativeMark Unstained Protein Ladder Reference

GelDoc-It TS Imaging

The UVP manual with VisionWorks Software was employed to capture fluorescent images of the gels obtained via electrophoresis (GelDoc-IT TS Imaging System; Ultraviolet Products LTD. Upland, CA). Each gel was carefully placed on the transilluminator surface within the darkroom of the system, covered by a small amount of distilled water. The overhead white light was turned on “Hi” and the system was set to “Autofocus” to obtain images. Images were taken at the automatic lens distance and by zooming in closer for better resolution for each gel using the VisionWorks software to adjust the parameters.

Bradford Assay

The Bradford protein assay method (Thermo Scientific Pierce Coomassie (Bradford) Protein Assay Kit; Thermo Scientific, Waltham, MA) was used to test the protein concentration of each ultracentrifuged almond protein isolate and salt sample solution. Directions from the ThermoFisher manual were used to prepare dilutions of the bovine serum albumin (BSA) calibration standard into ampules with a working range of 100-1500 ug protein / mL in alignment with the standard test tube and microplate protocols.[13] The Coomassie Reagent was equilibrated to room temperature and mixed before 1.5mL was added to 30uL of each sample in test tubes and the samples were incubated for 10 minutes at room temperature. The spectrophotometer (Genesys 10S UV-VIS, Thermo Scientific, Waltham, MA) was zeroed using distilled water and each diluted standard was measured at 595 nm to create a standard curve. The measurement for the blank replicate was subtracted from the other samples and results were graphed to determine a line of best fit. The standardization was performed in duplicate to obtain a higher coefficient of determination value and therefore better correlation. The initial standard curve coefficient of determination (r^2) was 0.9211 **(Figure 26)**, while the repeated curve had an improved value of 0.974 **(Figure 27).** Once the standard measurements were obtained, the absorbance at 595nm was also taken for each sample to determine total protein content. The initial measurements were out of range of the standard and each sample was diluted at a 1:1 ratio to improve the accuracy of results.

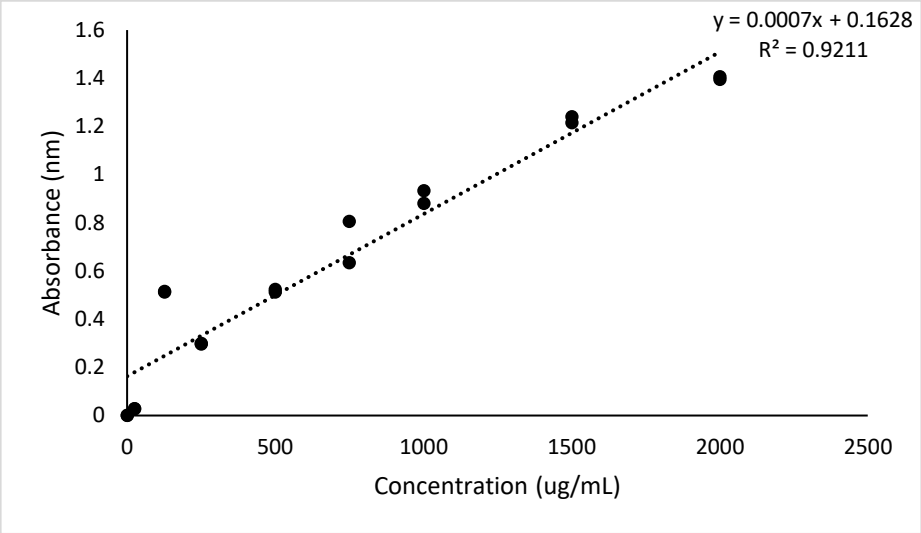

Figure 26. Standard Curve A of BSA

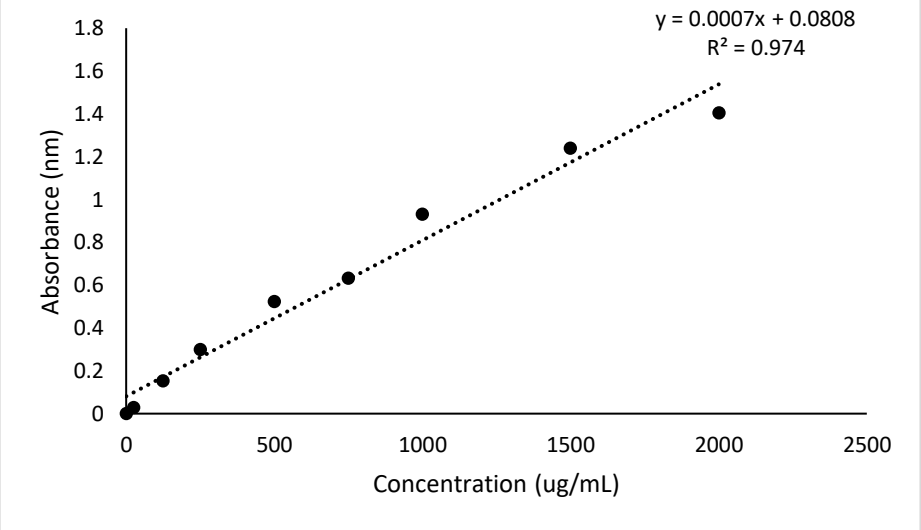

Figure 27. Standard Curve B for BSA

Results and Discussion

Effects of Sodium Citrate on APP Fluorescence

As seen in **Figure 28**, the trend in APP fluorescence with increasing salt content among the three almond protein powders was similar. The excitation wavelength for each replicate was 350 nanometers with an emission detected at 325 nanometers, meant to target the amino acid tryptophan. Increasing the sodium citrate concentration caused an initial decrease in fluorescence followed by a rise in detected fluorescence at *ca.* 10 mM salt content. The increase of tryptophan fluorescence at higher salt content (>10 mM) was probably due to the breakdown in protein quaternary structure, exposing the hydrophobic tryptophan residues typically harbored inside the core of the protein structure to the excitation as fluorophores. The protein types resulted in greater differences in results than expected, as APP 1 had the clearest data trends, with both APP 2 and 3 showing slightly different behavior. This may be due to differences in protein extraction protocols between companies, resulting in powders with unique protein composition and structure. Additionally, the variability between replicates of the same protein powder, seen here as the error bars for **Figure 28,** indicated that the CMU exhibited strong variability. Under the same temperature and salt conditions, each protein type (APP 1, APP 2, and APP 3) was expected to exhibit less variability in their fluorescence spectra. This was not the case, likely because the CMU is still a newly developed prototype with room for improvement for precision in the future.

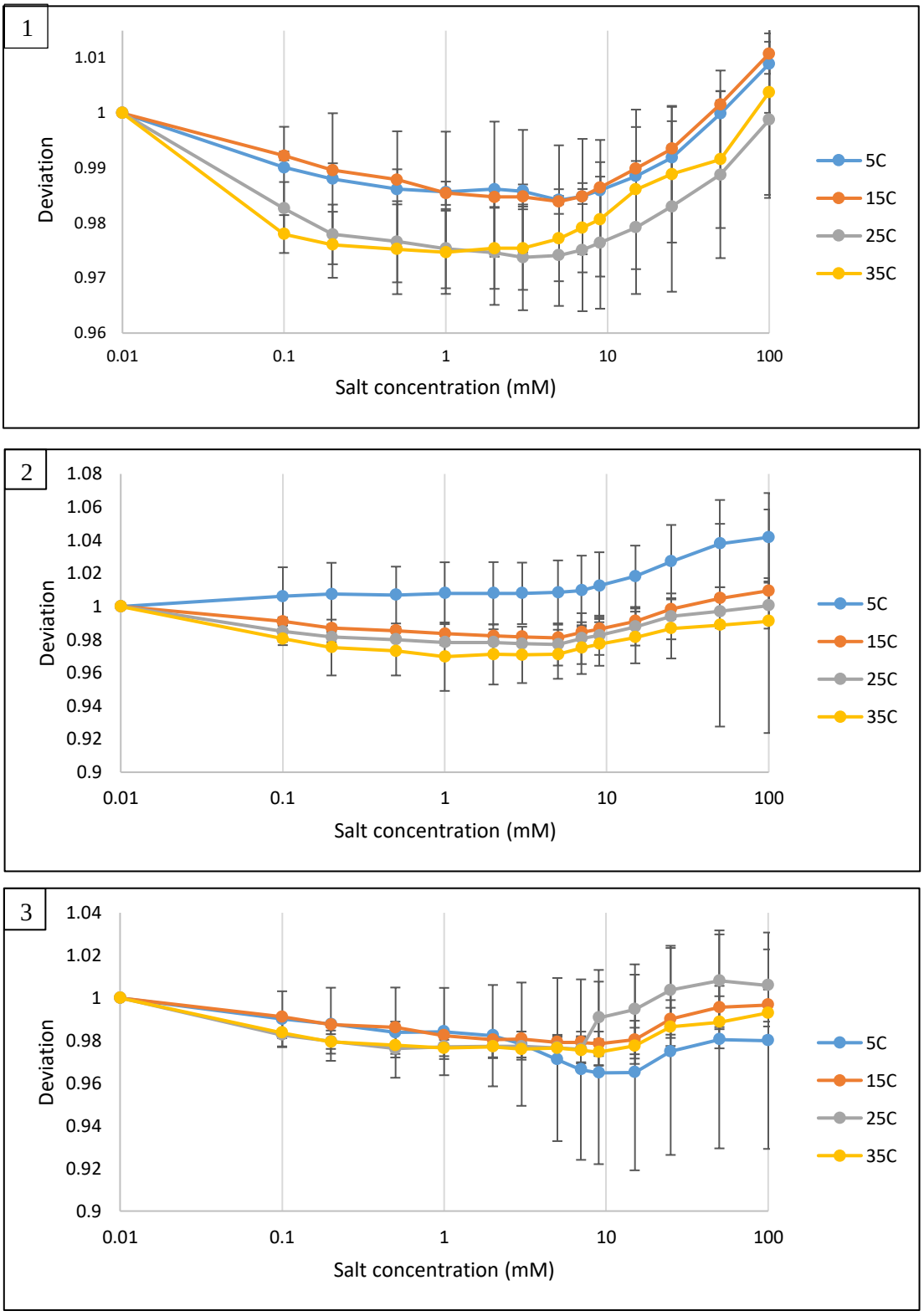

Figure 28. Deviation* of Fluorescence Values for APP 1, 2, and 3 from CMU Replicates

Effects of Sodium Citrate on APP viscosity

The pressure as the liquid samples were pumped through the flowcell was recorded as an indirect measure of viscosity. Decreased pressure readings indicated a corresponding reduction in viscosity of the protein-salt solution. For each protein dispersion and temperature combination, the pressure reading was found to decrease in pairing with the increasing salt concentration, as seen in **Figure 29**. This indicated that viscosity was dependent on both the temperature and salt concentration of the solution. This effect was the greatest for APP 1 **(Figure 29 A)**, which decreased by over *ca.* 15% for the sample held at 25°C. It was unexpected for the at 25°C APP sample to have a slightly larger effect than the 35°C APP sample, as the highest temperature would be more likely to have the most extreme effect on viscosity. For all APPs, the observed reduction in pressure suggested that the sodium citrate was effective in disrupting the quaternary structure of the natural almond protein. Instead of presenting as folded subunits, the proteins dissociated into small fragments. This effect was the opposite of what would occur for protein denaturation, which instead tends to increase the viscosity of solutions.[6]

APP 3 samples showed the least variation, as the error bars based on the percent deviation were the smallest among the three APP powders tested as seen in **Figure 29 C**. While APP 1 displayed the greatest difference in viscosity, it also had the largest error of the three APPs tested. Once again, this indicated that the CMU showed low repeatability and precision to detect the relatively small change in viscosity observed when increased concentration of salt was added to the protein dispersions.

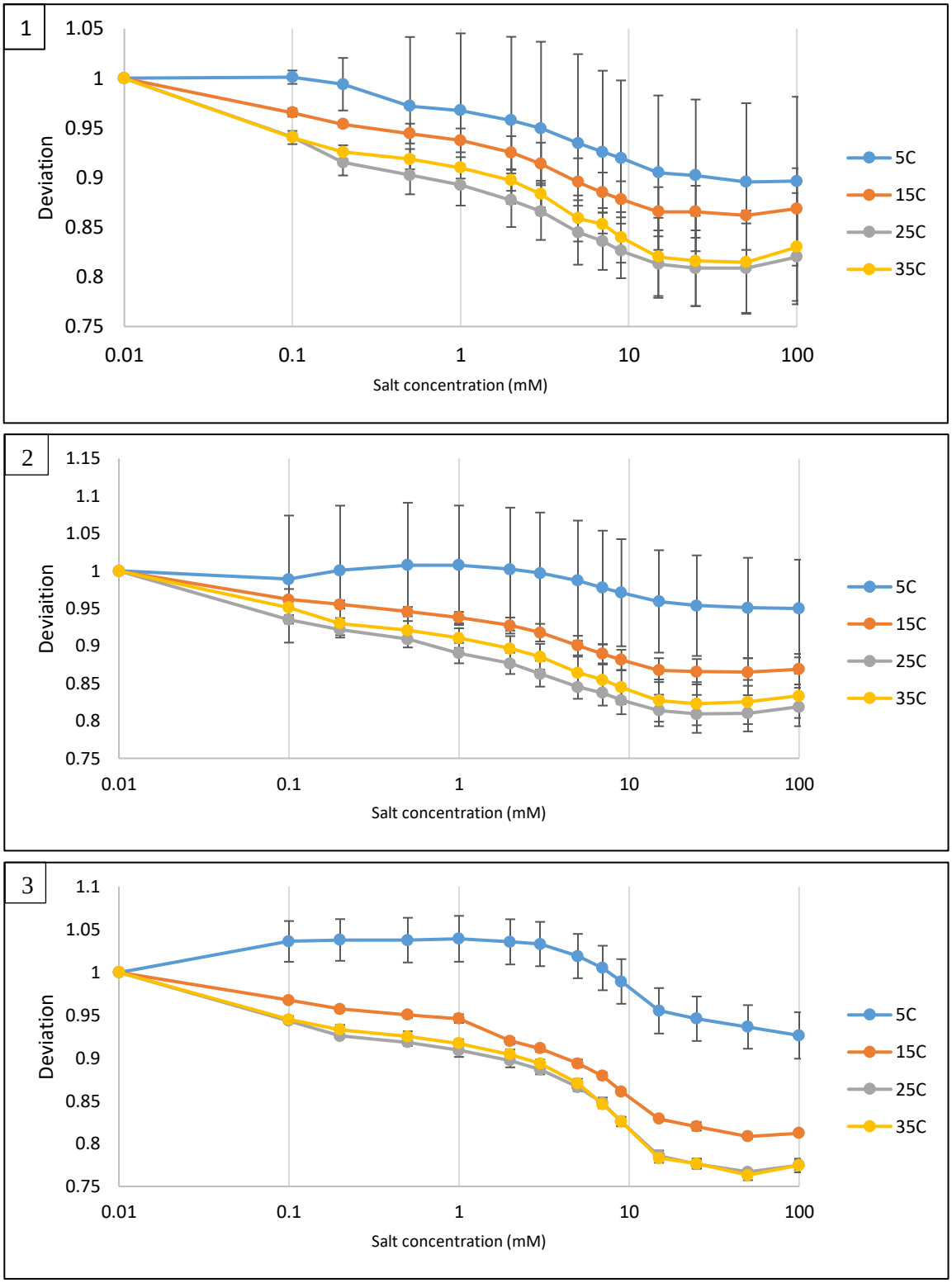

Figure 29. Deviation of Pressure Values of APP 1, 2. 3 from CMU Replicates

Protein Characterization by SDS-PAGE

The molecular weight disruption in almond protein isolates with increasing concentrations of sodium citrate was further proven using SDS-PAGE gel electrophoresis on ultracentrifuged samples. The molecular weight of the various APP proteins was estimated using the NativeMark LC0725 protein ladder (Invitrogen; Waltham, MA). As the salt concentration increased, more bands were visible for each APP within the gel. Visible in **Figure 30**, as the concentration of sodium citrate increased to 15 mM from 1 mM, the bands' distribution greatly changed. The darkest band appeared at around *ca.* 20 kDa at a salt concentration of 0.1-15 mM and correlated to the weight of the basic polypeptide of the most prevalent protein in almonds, amandin.[6] At salt concentrations above 15 mM, this protein started to disappear, with the band at *ca.* 40 kDa indicating a protein of higher molecular weight became more prevalent. This *ca.* 40 kDa band was a similar weight to the acidic polypeptide of amandin, expected to weigh between 39-42 kDa.[6] These polypeptides were visible distinctly due to the presence of the reducing agents SDS and β-mercaptoethanol, which broke the overall structure of the 60 kDa amandin protein (weight determined by amino acid sequence) into the two polypeptides.[6] At salt concentrations above 15 mM, multiple new bands appeared in the range of *ca.* 22-28 kDa. These likely represented the minor proteins present in almonds, making up 40% of the overall protein weight.[6] This effect continued with the increase in concentration to 100 mM, where the lower molecular weight bands nearly disappeared and multiple new bands at *ca.* 60-70 kDa became visible. These bands indicated that large protein aggregates (>250 kDa) were dispersed due to the action of high salt content in the samples. Between the three APP tested, APP 1 **(Figure 30)** showed the most significant results with increasing salt concentration, as the newly appearing bands were easily seen in comparison to lanes corresponding to the lower salt concentrations.

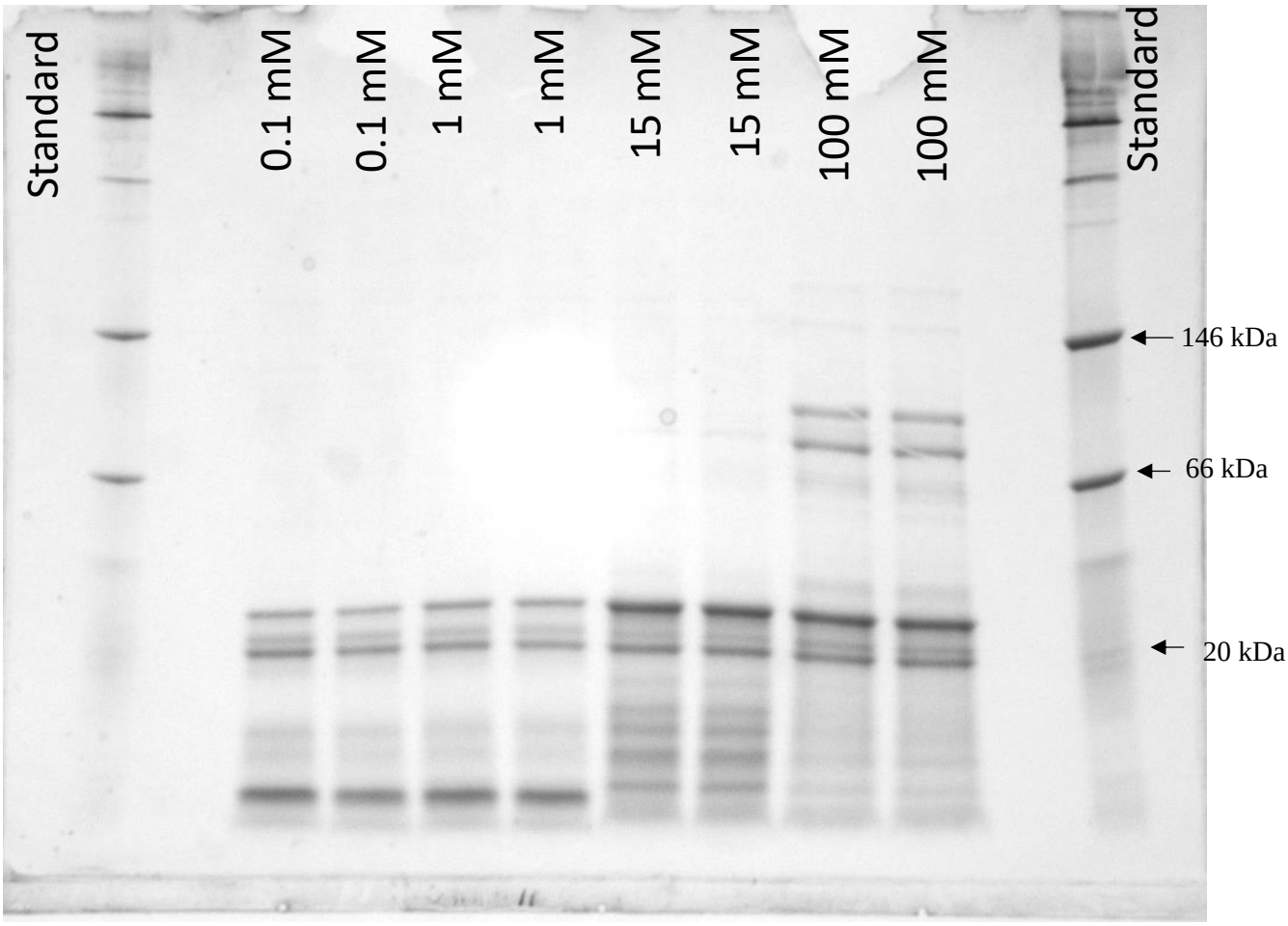

Figure 30. Gel Electrophoresis for APP 1

As shown in **Figure 31,** the effect of increasing salt concentration for APP 2 was similar to that of APP 1. Again, the smaller molecular weight components decreased in prevalence with increasing salt concentration in correspondence to the newfound presence of higher molecular weight protein units. The highest molecular weight components, having a mass of approximately *ca.* 50 kDa, had a lower intensity than those seen in APP 1 **(Figure 30)**, but still appeared at salt concentrations of 15 mM and above. The presence of medium-weight proteins (16 to 18 kDa) also became greatly more pronounced at a salt concentration of 15 mM. Unlike **Figure 30**, a faint shadow of a band appeared near 20 kDa in **Figure 31**. The stated hypothesis of increasing salt concentrations allowing for the change from a dispersion of larger protein aggregates to

smaller subunits becoming present was supported by this gel. The difference in almond protein powder processing and almond varietal types likely led to the variation between gels with subunits of varying molecular weights appearing.

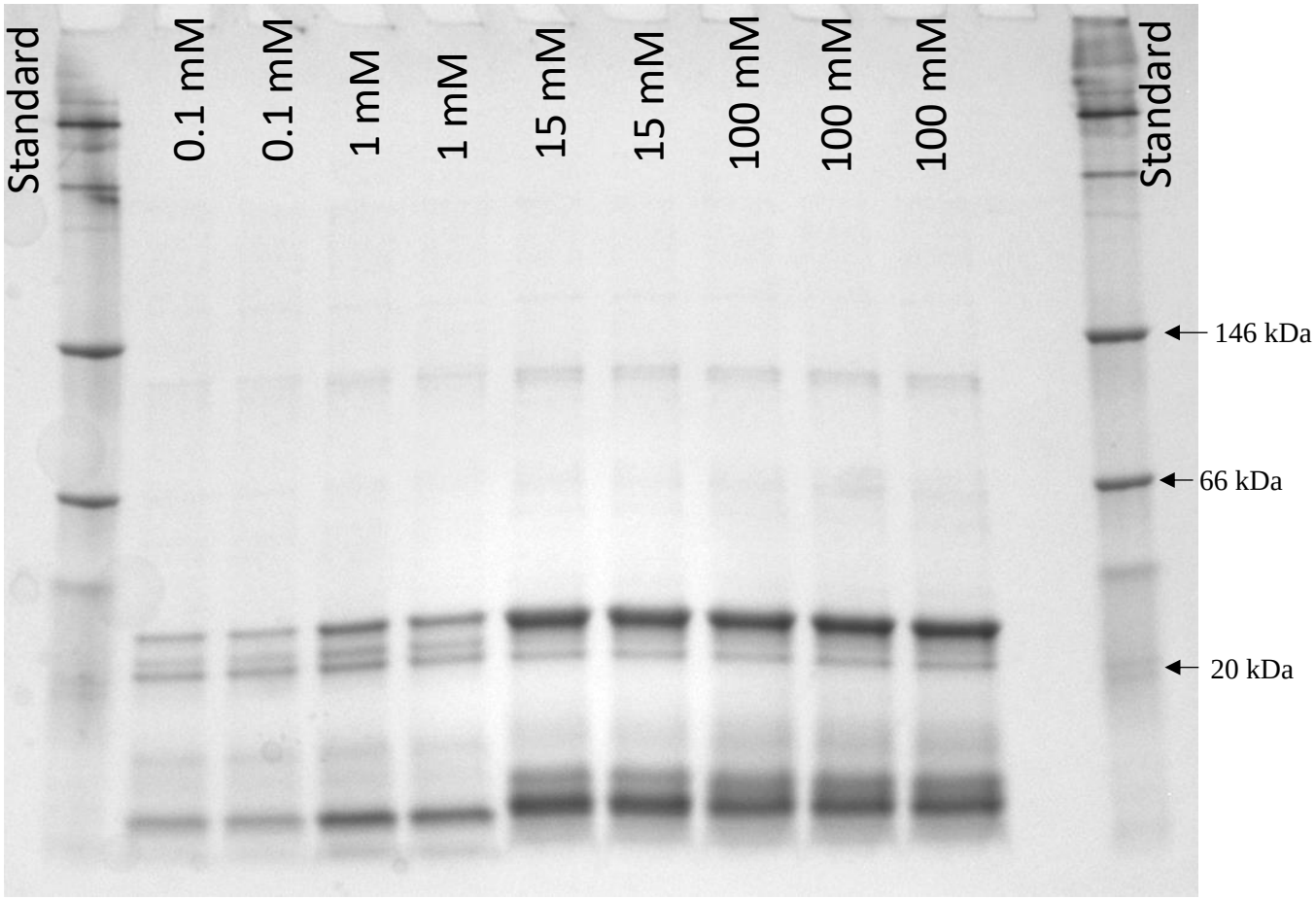

Figure 31. Gel Electrophoresis for APP 2

APP 3, as seen in **Figure 32**, exhibited similar behavior to APP 1 and 2 with increasing concentrations of higher molecular weight aggregations of approximately *ca.* 50 kDa present especially at a concentration of 100 mM of sodium citrate. Unlike the first two APP, APP 3 exhibited the highest molecular weight band at approximately *ca.*100 kDa in all gel lanes independent of salt concentration. While the band at *ca.* 50 kDa did appear at 100 mM of sodium citrate only, the protein subunits of APP 3 seemed to be affected less by sodium citrate than the

other two tested powders. Again, the presence of the larger protein subunit at about 100 kDa only appeared in **Figure 322**, aligning with the hypothesis that the processing and type of almond used to create the APP affected the results between powders.

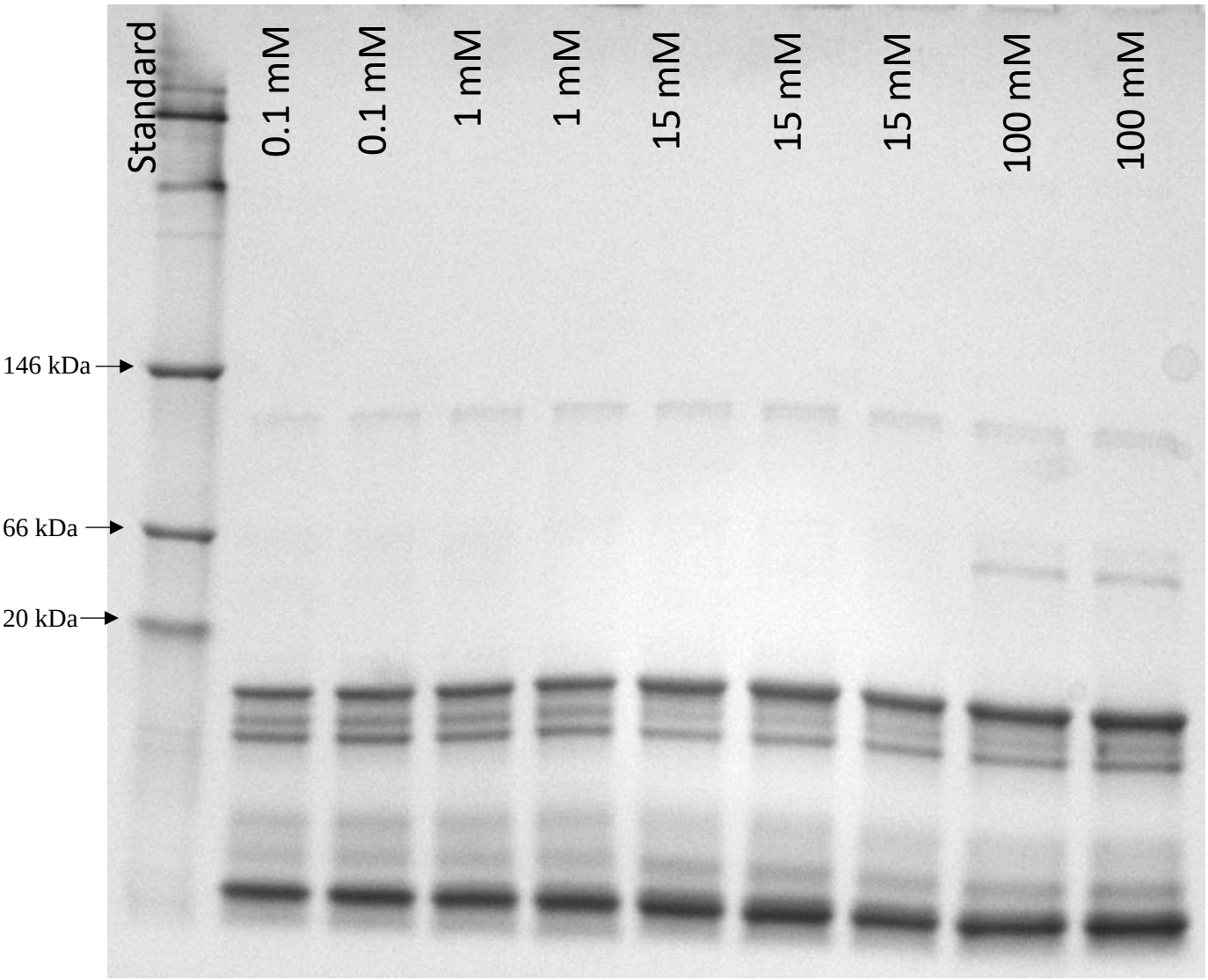

Figure 32. Gel Electrophoresis for APP 3

The results indicate that larger protein complexes may have been present in each APP solution regardless of salt concentrations, but that higher concentrations of sodium citrate (or potentially other emulsifying salts) were successful in solubilizing and dispersing these larger

molecular weight aggregates into smaller subunits. Additionally, since the reducing conditions would have successfully broken ionic interactions due to the presence of SDS and β-mercaptoethanol, the newly dispersed aggregates must be organized via a different structure. An alternative explanation would be that new covalent bonds are formed at high salt concentrations, but this has not been seen in previous literature and is unlikely to be the case.

Effects of Sodium Citrate on CMU Absorbance

Along with recording fluorescence and pressure, the CMU also detected the solution's absorbance using a deuterium lamp **(Figure 2 & 2)** connected to a flowcell and a UV-VIS absorbance spectrophotometer (**Figure 2)**. This was meant to provide data regarding the turbidity of the solution, as a higher absorbance reading indicated higher protein aggregation. A clear trend was seen in the initial replicates taken, such as the absorbance of APP 1 seen in **Figure 33**. In this case, the absorbance decreased with increasing salt concentration and temperature, suggesting that the solution was less turbid due to the dissociation of protein quaternary structures. However, reoccurring problems throughout later replicates caused the absorbance measurements from the CMU to be too variable. After examining the system, the deuterium lamp was found to be faulty. This caused the detected absorbance intensity to be abnormally low for all temperatures as seen in **Figure 34** and other replicates across different APP samples. The resulting data also exhibited a lot of noise instead of clear trends and was determined to be unreliable. Absorbance measures were instead measured externally to the CMU with the Bradford assay.

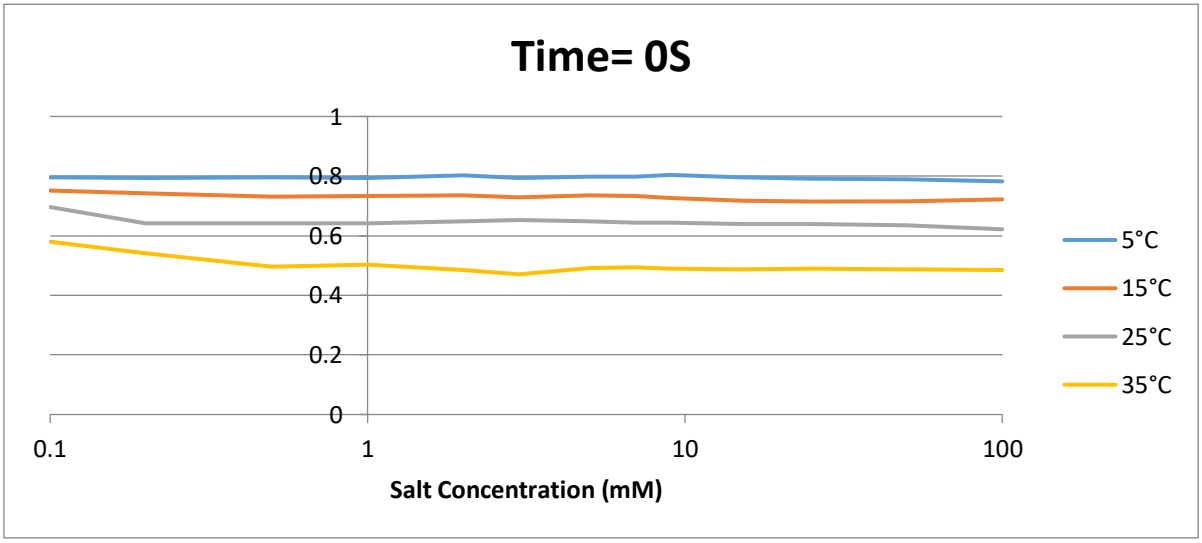

Figure 33. Absorbance of APP 1, Replicate 3

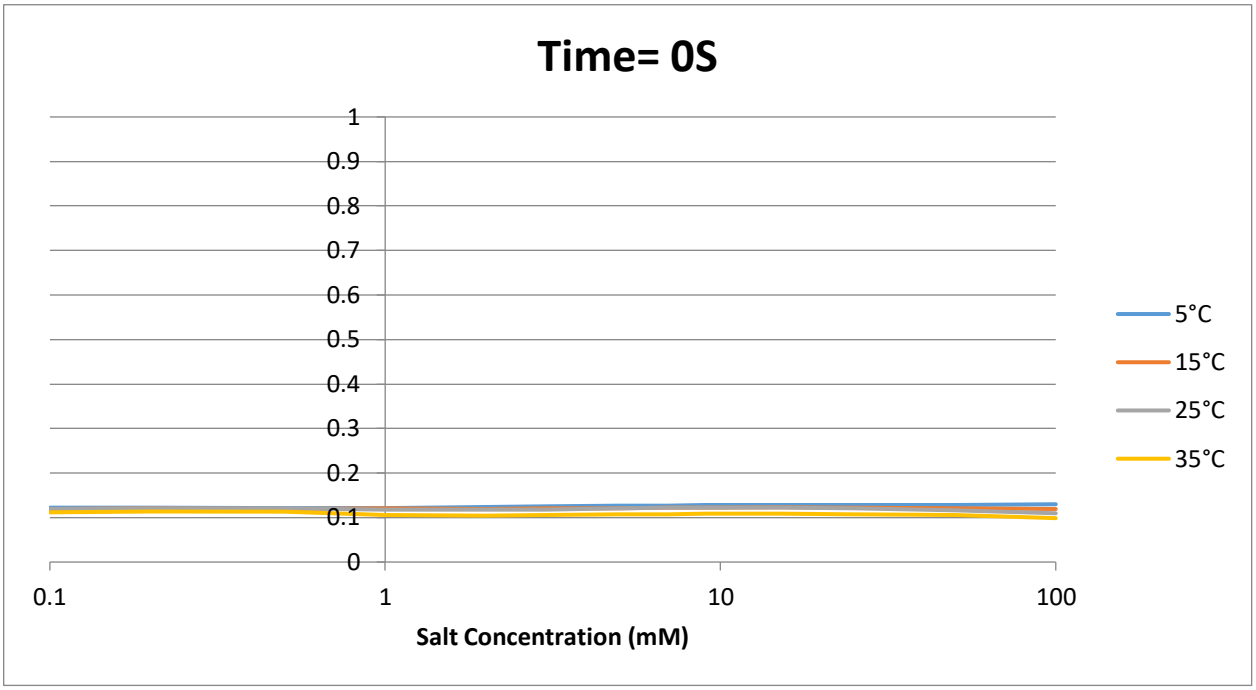

Figure 34. Absorbance of APP 3, Replicate 1

Bradford Assay Absorbance

The Bradford assay was used to measure the concentration of protein present by means of spectrophotometry following the addition of the Bradford reagent to each solution. Higher absorbance values corresponded to increased turbidity of solutions, as the concentration of salt was able to break down the APP protein quaternary structure. As seen below in **Figure 35**, the results appeared to be similar to the SDS-PAGE gels. The Bradford assay showed the largest change between 1.0-15 mM of salt concentration, as the absorbance of the APP 1 dispersions changed from 1,563 to 2,283 ug/mL, respectively. Since larger protein aggregates were able to disperse into solution at the higher salt concentrations, this caused the resulting increase in absorbance.

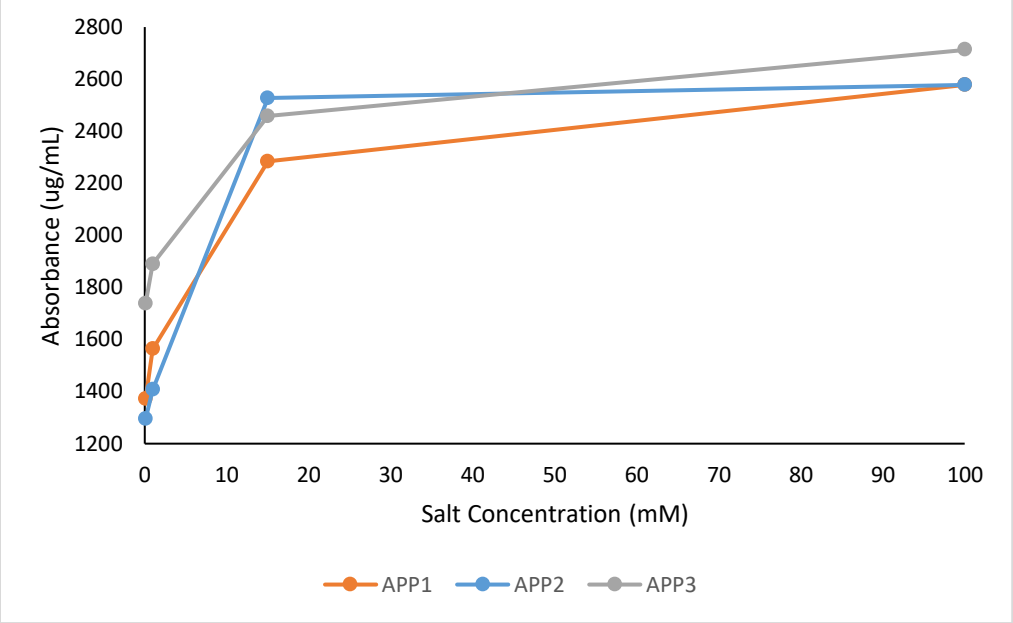

Figure 35. Calculated APP Absorbance from Bradford Assay

As absorbance is another measure of turbidity, this also suggests that the solutions became more turbid as the salt concentration increased due to the different protein aggregates that were soluble. The salt and APP combinations were recreated outside the CMU and results aligned, proving that the data from each output seemed accurate and reliable **(Figure 36)**.

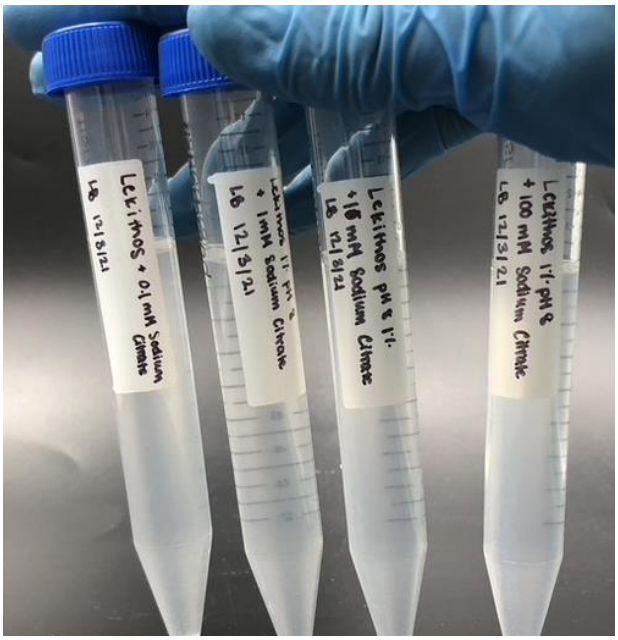

Figure 36. Turbidity of APP1 with Increasing Salt Concentrations

Chapter 4

Conclusion

As a commonly used emulsifying salt for plant-based beverages, sodium citrate had a limited effect in changing the distribution of protein aggregates and therefore the stability of almond-based solutions. For this work, three almond protein powders were reconstituted and adjusted to the pH 8 to mimic almond "milks" currently sold to consumers from brands such as Silk and Almond Breeze. These plant-based milks commonly add emulsifying salts with the intent to stabilize the beverage; however, the effects of these additions had not been previously researched. Although the changes appeared to be extreme via electrophoresis and the Bradford assay, they were less pronounced when measuring fluorescence and pressure. To determine changes in pressure and fluorescence, a newly developed CMU was used to mix and examine a range of temperatures and salt concentrations. As the CMU had not previously been described in a SOP, a thorough document was created to explain its use and cleaning procedures. As a prototype, this instrument was found to be unreliable when measuring absorbance with its own flowcell. Instead, the Bradford assay was used with an external spectrophotometer to collect this data. Sodium citrate seemed to affect the size and makeup of the protein aggregates as higher salt concentration solutions were less likely to show individual basic and acidic peptides of amandin via electrophoresis and instead had larger potential aggregates dispersed into solution, proven by the Bradford assay.

Overall, while this research did explore an area of plant-based milk stability that had previously been unknown, it left additional questions unanswered about the role of emulsifying salts for protein stability. As plant-based products continue to rise in popularity and expand items available in product lines, further work in this field could improve understanding.

BIBLIOGRAPHY

(1) Kundu, P.; Dhankhar, J.; Sharma, A. Development of Non Dairy Milk Alternative Using Soymilk and Almond Milk. *Curr. Res. Nutr. Food Sci. J.* **2018**, *6* (1), 203–210. https://doi.org/10.12944/CRNFSJ.6.1.23.

(2) McCarthy, K. S.; Parker, M.; Ameerally, A.; Drake, S. L.; Drake, M. A. Drivers of Choice for Fluid Milk versus Plant-Based Alternatives: What Are Consumer Perceptions of Fluid Milk? *J. Dairy Sci.* **2017**, *100* (8), 6125–6138. https://doi.org/10.3168/jds.2016-12519.

(3) Dairy Alternatives Market by Source (Soy, Almond, Coconut, Oats, Rice, Hemp), Application (Milk, Yogurt, Ice Creams, Cheese, Creamers), Distribution Channel (Supermarkets, Health Food Stores, Pharmacies), Formulation, and Region - Global Forecast to 2026, 2021.

(4) Ahrens, S.; Venkatachalam, M.; Mistry, A. M.; Lapsley, K.; Sathe, S. K. Almond (Prunus Dulcis L.) Protein Quality. *Plant Foods Hum. Nutr.* **2005**, *60* (3), 123–128. https://doi.org/10.1007/s11130-005-6840-2.

(5) Lewis, G.; Bodinger, L. R.; Harte, F. M. Characterization of Ethanol-Induced Casein Micelle Dissociation Using a Continuous Protein Monitoring Unit. *J. Dairy Sci.* **2022**, *105* (9), 7266–7275. https://doi.org/10.3168/jds.2021-21522.

(6) Devnani, B.; Ong, L.; Kentish, S.; Gras, S. Heat Induced Denaturation, Aggregation and Gelation of Almond Proteins in Skim and Full Fat Almond Milk. *Food Chem.* **2020**, *325*, 126901. https://doi.org/10.1016/j.foodchem.2020.126901.

(7) Trade, N. Z. M. of F. A. and. *Milk alternatives popularity growing in the US - February 2022*. New Zealand Ministry of Foreign Affairs and Trade. https://www.mfat.govt.nz/en/trade/mfat-market-reports/market-reports-americas/milk-alternatives-popularity-growing-in-the-us/ (accessed 2022-11-30).

(8) *Milk and Non-dairy Milk - US - 2021: Market Share*. https://reports-mintel-com.ezaccess.libraries.psu.edu/display/1099709/?fromSearch=%3Ffreetext%3Dalmond%2520milk&resultPosition=1 (accessed 2022-12-06).

(9) Norton, G. *Plant Proteins: Easter School in Agricultural Science*; Butterworth-Heinemann, 2013.

(10) Burstein, E. A.; Vedenkina, N. S.; Ivkova, M. N. Fluorescence and the Location of Tryptophan Residues in Protein Molecules. *Photochem. Photobiol.* **1973**, *18* (4), 263–279. https://doi.org/10.1111/j.1751-1097.1973.tb06422.x.

(11) Sorvall MTX 150 Micro-Ultracentrifuges - Instruction Manual.

(12) *Performing Protein Electrophoresis*. Bio-Rad Laboratories. https://www.bio-rad.com/en-us/applications-technologies/performing-protein-electrophoresis?ID=LUSPFBNEL (accessed 2023-03-06).

(13) *Pierce™ Coomassie (Bradford) Protein Assay Kit*. https://www.thermofisher.com/order/catalog/product/23200 (accessed 2023-03-30).

(14) *Heat induced denaturation, aggregation and gelation of almond proteins in skim and full fat almond milk | Elsevier Enhanced Reader*. https://doi.org/10.1016/j.foodchem.2020.126901.

ACADEMIC VITA

Education

The Pennsylvania State University, Schreyer Honors College, University Park, PA
B.S. in Food Science | Minor in Nutritional Sciences

Work Experience

R&D Intern, The Hershey Company | May 2022-August 2022

- Developed and refined formulas for four innovation concepts to assess components for product delivery, cost, shelf life, and profitability
- Conducted an analytical and sensory competitor category review to understand consumer insights for future product launches
- Compiled data to create a concise reference document for product developers
- Supported benchtop and pilot plant runs to prepare products for national consumer testing

Consumer Foods R&D Intern, Smucker Natural Foods, The J.M. Smucker Co. | May 2021 -August 2021

- Formulated new natural and organic juice blends using functional and trending ingredients for national brands including R.W. Knudsen, Santa Cruz Organics, and Trader Joe's
- Presented prototypes to cross-functional team at product cuttings for feedback and review
- Achieved proficiency with formulation strategies, lab practices, & tools
- Executed microbiome research through company interviews & advised for future product launches

Research Assistant, Dr. Federico Harte's Dairy Protein Laboratory, Penn State | August 2020-Present

- Research and publish honors thesis concerning interactions between almond proteins and emulsifying salts affecting the viscosity and functionality of almond protein beverages
- Conduct literature reviews of professionally published research
- Analyze weekly presentations to further understand research methods and technology

Resident Assistant, North Halls, Pennsylvania State University| August 2021-Present

- Counsel and advise students for social, academic, and personal conflicts
- Implement creative programming to promote a positive and inclusive community for 71 residents

Sensory Technician, Penn State Sensory Evaluation Center | October 2019-March 2020

- Prepare laboratory samples for consumer sensory testing
- Maintain optimal testing conditions to reduce confounding variables

Leadership

Food Science Club, President (Previous Vice President, Public Relations Chair) | January 2021-Present

- Coordinate presentations by international food companies for networking and career opportunities
- Implement new annual Club Banquet to highlight successes of department and individuals
- Collaborate with executive board to fundraise and plan seasonal events

2020 Campus Hunger Project Cohort Leader | June 2020-Present

- Spearhead an initiative to bring national nonprofit Swipe Out Hunger to Penn State's campuses
- Communicate professionally with campus executives to implement and publish effective plans
- Strategize with a national team of leaders to enact long-lasting change

Challah for Hunger, President (Previous Vice President, Secretary) | January 2020-Present

- Organize bi-weekly events to support nationwide campus hunger-relief efforts
- Execute outreach, communication, and development strategies

Publications

Lewis, G., Bodinger, L. R., Harte F.M. Characterization of ethanol-induced casein micelle dissociation using a continuous protein monitoring unit. Journal of Dairy Science. Accepted for publication.

Awards

2023 Spring Graduation Department of Food Science Student Marshal
2021-Present Gamma Sigma Delta Agricultural Honors Society
2022-Present Phi Tau Sigma Food Science Honor Society
2021 and 2022 Judith A. Williams Food Industry Group Undergraduate Student Leadership Award
2022 IFT John and Irene Powers Award
2021 IFT Feeding Tomorrow McCormick & Company Scholarship
2021 and 2022 Keystone IFT Scholarship
2021 College of Agricultural Sciences Undergraduate Research Award
2020 Paul R. and Ethel S. Guldin Agricultural Award
2019-2023 Frank S. and Nina Cobb Grant-In-Aid
2019-2023 Edna May Aucker Scholarship
2019-2023 Galen Dreibelbis Endowment for Excellence in Agriculture
2019-2021 Harry Hayward Academic Excellence Scholarship